国内外前寒武纪条带状铁建造研究现状

代堰锫[1,2)],朱玉娣[3)],张连昌[2)],王长乐[2)],陈超[4)],修迪[4)]

1)中国地质调查局成都地质调查中心,成都,610081;2)中国科学院地质与地球物理研究所,北京,100029;3)西南石油大学地球科学与技术学院,成都,610500;4)河北省区域地质矿产调查研究所,河北廊坊,065000

内容提要:条带状铁建造(BIFs)主要发育于早前寒武纪时期(3.8~1.8Ga),记录了早期地球演化的重要信息且蕴含丰富的铁矿石资源。本文梳理总结了国内外BIF相关领域的研究认识及存在问题:① 统计对比显示,BIF沉积事件与地幔柱、地壳增生等重大地质事件相关;② 稀土元素及Nd同位素示踪表明,Fe来源于海水与海底高温热液的混合溶液,其中高温热液与海水比例为1:1000;③ BIFs缺乏负Ce异常且富集重Fe同位素,暗示沉积时古海洋整体处于缺氧环境以避免Fe^{2+}发生氧化;④ 一些重要科学问题尚未解决,例如Si的主要来源、沉淀机制及条带成因等;⑤ 华北克拉通BIFs多形成于约2.54Ga,BIF类型、形成时代与富矿成因等问题有待深入研究。本文认为,加强国内外典型BIFs的对比研究并适当应用现代先进测试技术,有利于探索BIF沉积的精细过程及古老克拉通的早期演化。

关键词:条带状铁建造;物质来源;沉淀机制;沉积环境;条带成因;形成时代

条带状铁建造(banded iron formations,简称BIFs)是指全铁含量大于15%,由富铁矿物(以磁铁矿或赤铁矿为主)和脉石矿物(以石英为主)组成的具有条带(纹)状构造的化学沉积岩(James,1954,1983)。BIFs在全球广泛发育,主要分布于南美、北美、格陵兰、非洲、澳大利亚、俄罗斯、中国、印度等地的古老克拉通内(Gross,1980,1983;Trendall,2009;Bekker et al.,2010);时代主要介于3.8~1.8 Ga(Huston and Logan,2004),尤以2.7~2.0 Ga最为发育(Klein,2005)。根据其形成时代及含矿建造,BIFs可分为两种类型:Algoma型主要产于太古宙,多形成于岛弧、弧后盆地或克拉通内裂谷带,与海底火山活动关系密切;Superior型主要产于古元古代,一般发育于浅海环境且与沉积作用密切相关,不含或含有极少量的火山岩,沉积规模远大于Algoma型(Gross,1980,1983,1996)。

BIFs是早前寒武纪时期地球特殊环境的产物,记录了当时地球深部、大气、海洋和生物等方面的重要信息(Bekker et al.,2010)。例如,Han and Runnegar(1992)在Negaunee BIF(约2.1 Ga)中识别出肉眼可见的藻类;Brocks等(1999)从Hamersley盆地页岩层萃取出碳氢化合物,认为是蓝藻进行光合作用的有力证据;Ribeiro and Crowley(2012)发现巴西Carajas BIF(约2.75 Ga)硅铁条带分别具瓣状(直径5~10 μm)及管状构造(直径0.5~5 μm),其碳同位素分析结果显示为生物成因($\delta^{13}C_{V-PDB}=-24.5‰$),表明BIFs的形成与微生物活动有关。显而易见,对BIFs的精细研究有助于了解地球生命的起源与演化。此外,BIFs蕴含丰富的铁矿石资源,占全球铁矿石总产量的90%以上(Isley,1995)。BIF型铁矿床被国内学者称为"鞍山式"铁矿(程裕淇,1957)或"沉积变质型"铁矿(陈光远等,1984),其资源量占中国铁矿石总储量约58%(Zhang Zhaochong et al.,2014)。毫无疑问,深入剖析BIF成矿作用能够为找寻铁矿资源提供丰富信息。因此,对BIFs的系统研究具有重要的科学意义与应用价值。

1 国际BIF研究现状

目前,国际上对BIFs的研究主要围绕5个方面开展,包括BIF相关重大地质事件、物质来源、沉淀机制、古沉积环境及条带成因。

注:本文为国家重点基础研究发展计划973项目(编号:2012CB416601)、四川省教育厅科研项目(编号:15ZB0058)和成都地质调查中心青年科学基金项目(编号:所控基[2015]-05)的成果。

收稿日期:2015-05-07;改回日期:2015-12-04;责任编辑:章雨旭。Doi:10.16509/j.georeview.2016.03.015

作者简介:代堰锫,男,1986年生。工程师,理学博士,矿床学专业。Email:diyeplas@foxmail.com。

1.1 重大地质事件

由于 BIFs 在世界上广泛发育,多数学者认为 BIFs 的沉积或消亡与全球性重大地质事件具有成因联系。

(1)大氧化事件:基于沉积硫化物与硫酸盐中的硫同位素非质量分馏效应(Farquhar et al. ,2000)、古土壤成分的变化(如铁的亏损,Rye and Holland,1998)以及氧化还原敏感矿物的消失(如沥青铀矿与黄铁矿,Ono et al. ,2000;Frimmel,2005)等证据,科学家发现地球大气圈 O_2 含量在古元古代早期明显增加并持续升至现代水平,称之为"大氧化事件"(Great Oxidation Event,简称 GOE,Holland,2002),发生时间为 2.4 ~ 2.2Ga(Kasting,1993,2001;Canfield,2005;Holland,2006)。由于 BIFs 沉淀过程需要将古海洋中大量存在的 Fe^{2+} 氧化为 Fe^{3+}(Cloud,1968;Holland,1973;Trendall,2009;Bekker et al. ,2010),因此部分学者认为 GOE 与 BIFs 形成之间可能存在某种联系(Klein,2005;Heck et al. ,2011;Zhai Mingguo and Santosh,2013)。然而,在 GOE 前漫长的地质历史时期,甚至远及 3.8Ga(如 Isua 与 Nuvvuagittuq BIFs),地球上同样发育大量 BIFs;此外,精细的年代学统计亦表明,GOE 并非对应于 BIFs 沉积高潮(Isley and Abbott,1999;Bekker et al. ,2010)。在 1.85Ga 之后,大气圈 O_2 浓度的增加使地球整体处于氧化环境,从而导致 BIFs 的消失(Canfield,1998;Huston and Logan,2004;Bekker et al. ,2010);新元古代末期的"雪球地球"事件(Snowball Earth events,0.8 ~ 0.6Ga,Hoffman et al. ,1998),使全球海洋再次处于缺氧环境并形成了 Rapitan 型 BIFs(Klein and Beukes,1993;Klein,2005;Bekker et al. ,2010;Halverson et al. ,2011)。综合,本文认为 BIF 沉积事件与 GOE 并无成因联系。甚至部分学者提出,BIFs 沉积过程耗氧量虽小但不能忽略不计(Holland,2006),因此 2.4Ga 以前的 BIFs 发育还可能延缓了 GOE 的发生(Kasting,2013)。

(2)地幔柱及大火成岩省:Isley(1995)及 Isley and Abbott(1999)发现全球 BIFs 沉积高峰与地幔柱活动具有良好的对应关系,认为地幔柱活动能够将大量 Fe 带入海洋,并提供全球缺氧环境及适合的构造背景(如洋底高原、海山及克拉通内裂谷),有利于 BIFs 的形成。Barley et al.(1997)指出 2.6 ~ 2.2Ga 为全球构造—岩浆活动静寂期,该时间段海洋中 O_2 含量逐渐增多,使得海水中溶解的 Fe^{2+} 减少并导致 BIFs 沉积速度缓慢;但澳大利亚 Hamersley BIF(2770 ~ 2405Ma,Müller et al. ,2005)巨厚沉积层中却夹杂了一套大于 30000km^3 的粒玄岩、玄武岩及流纹岩组合,表明大火成岩省就位可能是 Hamersley BIF 沉积的主导因素(Barley et al. ,1997,2005;Pickard,2002)。

(3)地壳增生:Zhai Mingguo and Windley(1990)系统研究了华北克拉通 BIFs 的时空分布及地球化学特征,认为这些 BIFs 及相关岩系的发育反映了太古宙的加积与地壳增生过程。Rasmussen et al. (2012)提出自 2.32Ga 开始全球 BIFs 的沉积处于低潮,但在约 0.5Ga 之后又出现了 BIFs 的沉积高潮;西澳大利亚 Frere Formation 中 BIFs(1.88Ga)与全球基性—超基性岩浆活动、新生地壳形成、地幔亏损及 VMS 形成时代相当,表明 BIFs 的沉积是地幔活动及地壳快速增生的结果,后者为 BIFs 的发育提供丰富的铁质来源及适宜的还原环境。

(4)板块构造:Kato 等(1998)研究西澳大利亚 Pilbara 克拉通 Cleaverville 地区 BIFs(3.3 ~ 3.2Ga)时,基于地质学、岩石学及地球化学证据,发现该套岩系保留了从洋中脊到汇聚板块边缘连续的沉积环境记录;他们认为这是板块运动的结果,并且提出板块构造体制至少在中太古代就已经启动。Dobson and Brodholt(2005)基于地球壳幔过渡带超低速区域(Ultralow-velocity zones,简称 ULVZs)的地球物理特征,提出 2.8 ~ 1.8Ga 期间沉积于洋底的 BIFs 可能会通过板块俯冲的方式进入地球内部从而形成 ULVZs。

(5)陨击事件:Slack and Cannon(2009)认为北美 Lake Superior 地区 BIF 沉积事件在 1.85Ga 之后突然中止,可能与 Sudbury 陨击事件(约 1.85Ga,Cannon et al. ,2010)有关;该事件造成全球浅部氧化海水与深部缺氧海水发生混合,最终导致深部海水处于次氧化状态并使得 Fe^{2+} 无法运移。Glikson and Vickers(2007)以及 Glikson(2010)发现在 8 个太古宙—古元古代陨石撞击沉积单元(impact fallout/ejecta units)中,5 个时代分别为 3.47Ga、3.26Ga、3.24 Ga、2.63 Ga 及 2.56 Ga 的沉积单元均上覆 BIFs;他们认为陨击事件引发基性岩浆活动及热液活动,为 BIFs 的形成带来丰富的 Fe。众所周知,BIF 沉积事件在全球普遍发育且持续时间漫长(3.8 ~ 1.8Ga,Huston and Logan,2004),陨击理论难以解释 BIFs 时空分布的广泛性。

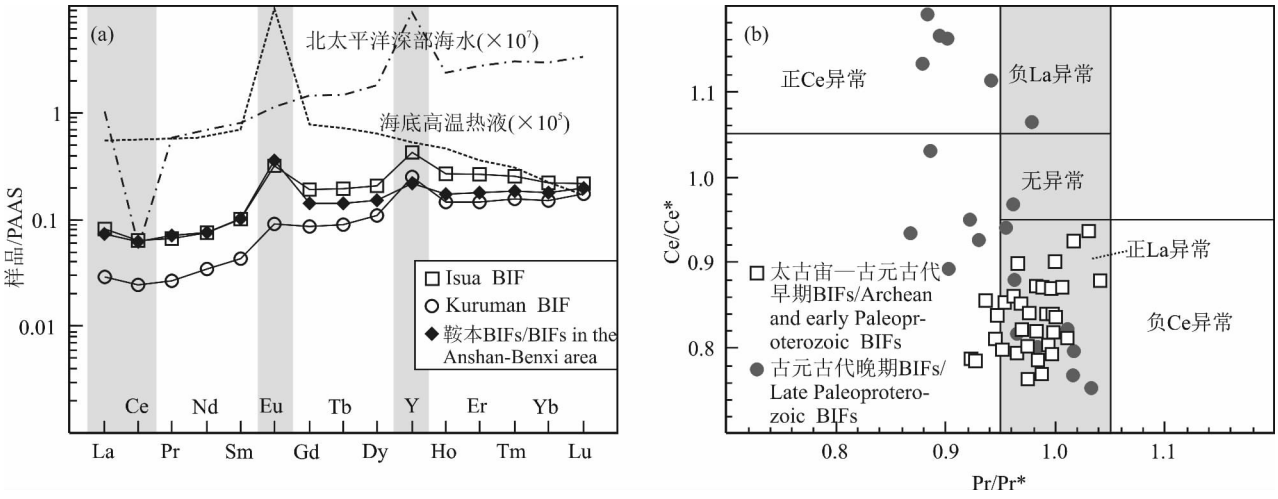

图 1 (a) BIFs 稀土元素 PAAS 标准化配分图,标准化数据引自 McLennan(1989),Isua 与 Kuruman BIFs 数据引自 Alexander 等(2008),鞍本 BIFs、北太平洋深部海水及高温热液数据分别引自代堰锫(2014)、Alibo and Nozaki(1999)、Bau and Dulski (1999);(b) Ce 异常判别图解,底图据 Bau and Dulski(1996),BIFs 数据引自 Bekker 等(2010)

Fig. 1 (a) PAAS-normalized REE patterns of BIFs, and the values of PAAS, Isua BIF, Kuruman BIF, BIFs in the Anshan—Benxi area, North Pacific deep water and high-T hydrothermal fluids after McLennan (1989), Alexander et al. (2008), Dai Yanpei (2014), Alibo and Nozaki (1999) and Bau and Dulski (1999), respectively; (b) Ce anomaly discrimination diagram after Bau and Dulski, 1996, and the data of BIFs after Bekker et al. (2010)

1.2　物质来源

Fe 与 Si 的物质来源历来是 BIFs 研究的核心问题之一(Cloud, 1973; Klein, 2005; Bekker et al., 2010)。Cloud(1973)鉴于 BIFs 与火山岩序列的共生关系,提出 BIFs 中的 Fe 属海底喷流成因(exhalative source)。Holland(1973)认为地球早期大洋深部海水较之浅部海水更富 Fe,深部海水的上涌可能是 BIFs 沉积于浅海区域的原因,意即 BIFs 中的 Fe 来自于海水。Jacobsen and Pimentel-Klose (1988a)研究 Hamersley 与 Michipicoten BIFs 时发现 Nd 同位素呈正值($\varepsilon_{Nd}(t)=4\sim0$),提出 Fe 主要源于地幔;Jacobsen and Pimentel-Klose(1988b)研究了 8 个不同时代 BIFs 的 Nd 同位素组成,发现 Urucum (0.65 Ga)与 Gunflint(1.9 Ga)BIFs 的 $\varepsilon_{Nd}(t)$ 介于 $-6.1\sim0$ 之间,而其它 BIFs(3.4 ~ 1.84 Ga)的 $\varepsilon_{Nd}(t)$ 为 $-1.0\sim-4.0$;认为太古宙 BIFs 中的 Nd 为亏损地幔来源,暗示太古宙海水中 REEs 主要来自洋中脊热液。Rao and Naqvi(1995)基于 Chitradurga 片岩带产出的 BIFs 具有强烈的 Eu 正异常,提出 Fe 主要来自海底高温热液。

REEs 具有非常稳定的地球化学性质,是研究地质过程与物质来源的重要工具(Kato et al.,1998)。相关实验结果业已证实,Fe 与 REEs 在运移及沉淀过程中不会发生分异(Bekker et al.,2010)。因此,近年来稀土元素被广泛应用于示踪 BIFs 中 Fe 的物质来源。地质学家发现,全球典型 BIFs 基本均显示富集重稀土、La 正异常、Y 正异常及高于球粒陨石的 Y/Ho 比值(图 1a),这些特征与现代海水 REE 特征吻合(Zhang et al., 1994; German et al., 1995; Alibo and Nozaki,1999)。此外,BIFs 还具有强烈的 Eu 正异常特征,与海底高温热液特征一致($t>350$ ℃,Klinkhammer et al.,1994; Bau and Dulski,1999; Douville et al.,1999)。因此,地质学家目前普遍认为 BIFs 中的 Fe 来源于海水与海底高温热液的混合溶液(Bau and Dulski,1996; Khan et al.,1996; Bolhar et al.,2005; Klein,2005; Bekker et al.,2010),这一认识同样为 Nd 同位素证据所支持(Jacobsen and Pimentel-Klose,1988a,1988b; Alibert and McCulloch, 1993; Bau et al.,1997)。据 Alexander 等(2008)介绍的二元混合模型,原始混合溶液中海底高温热液比例仅约 0.1% 即能产生足够的 Eu 正异常。

实验研究表明地球不同储库的 Fe 同位素组成有差异:BIFs 呈现富集 Fe 的重同位素基本特征($\delta^{56}Fe_{IRMM}>0$, Johnson et al., 2008; Steinhoefel et al., 2009; Planavsky et al.,2012),碳酸盐岩、海水、河水及洋中脊热液富集 Fe 的轻同位素($\delta^{56}Fe_{IRMM}<0$, Dauphas et al., 2007; Bergquist and Boyle, 2006; Severmann et al.,2004; 孙剑和朱祥坤,2015),地幔

包体与岩浆岩集中于零值附近(Weyer and Ionov, 2007)。这种差异主要是由于地幔熔融与结晶分异过程 Fe 同位素分馏程度较小,而氧化还原过程 Fe 同位素会发生较大分馏,并且在三价铁相中富集 Fe 的重同位素、在二价铁相中富集 Fe 的轻同位素(Johnson et al. ,2002)。Johnson 等(2008)认为前寒武纪热液摄入量与热流更高、氧化效率更低,因此当时海底高温热液的 Fe 同位素组成应该更接近于洋壳($\delta^{56}Fe_{IRMM}=0$),与现代海底高温热液具有较低的 $\delta^{56}Fe_{IRMM}$ 值不同(-0.6‰ ~ -0.2‰, Severmann et al. ,2004)。据此,Steinhoefel 等(2009)将前寒武纪 BIFs 富集 Fe 的重同位素特征($\delta^{56}Fe_{IRMM}>0$)解释为海底热液成因,并认为 $\delta^{56}Fe_{IRMM}$ 值的高低与当时海底热液活动的强弱有关。

Si 同位素无疑是示踪 BIFs 中硅质来源最为直接的手段。海底高温热液 $\delta^{30}Si_{NBS-28}$ 值以现代海底黑烟囱为代表,介于 -0.38‰(地幔, Georg et al. , 2007)与 -3.1‰(Mariana 海沟热液口, Wu Shiying et al. ,2000);陆源风化产物 $\delta^{30}Si_{NBS-28}$ 值较高,如玄武岩大于 -0.5‰(Ziegler et al. ,2005; Bern et al. , 2010),长英质火山岩为 -0.07‰ ±0.05‰,片麻岩、麻粒岩与混合岩为 -0.10‰ ±0.15‰,石英岩与砂岩为 0.02‰ ±0.05‰(André et al. ,2006)。Heck 等(2011)统计了 Isua(3.8Ga)、Hamersley(2.5Ga)、Transvaal(2.5Ga)以及 Biwabik(1.9Ga)BIFs 的 Si 同位素组成,225 个分析点的 $\delta^{30}Si_{NBS-28}$ 值介于 -3.7‰ ~ 1.2‰;他们认为 BIFs 中的 Si 主要来自海底高温热液($\delta^{30}Si_{NBS-28}<-0.38‰$),同时也有少量陆源硅质组分($\delta^{30}Si_{NBS-28}>-0.38‰$, 约 40 个分析点)的加入。Hamade 等(2003)研究了西澳大利亚 Dales Gorge BIF(2.5Ga)的 Ge/Si 比值,发现随着 Si 含量增高,Ge/Si 比值明显降低,趋向于陆源风化端元(continental end member);当 Si 含量降低时,Ge/Si 比值显著升高,更靠近热液来源端元(hydrothermal end member)。他们认为 BIFs 沉积过程中 Fe 与 Si 的来源不同:Fe 主要源于海底高温热液,Si 则主要来自陆源风化产物(Hamade et al. , 2003)。众所周知,由于 Al_2O_3 与 TiO_2 不能被溶液引入,二者常被用于示踪 BIFs 中陆源碎屑物质的混染程度(Pecoits et al. ,2009; Basta et al. ,2011)。前寒武纪 BIFs 普遍具有较低的 $Al_2O_3+TiO_2$ 含量,例如南非 Pongola BIF 该值平均仅为 0.32%(Alexander et al. ,2008),暗示 BIF 沉积过程陆源碎屑物质加入量较少(Pecoits et al. ,2009; Basta et al. ,2011; Dai Yanpei et al. ,2014; Lan Tingguang et al. ,2014a),与 Heck 等(2011)的 Si 同位素分析结果一致。

1.3 沉淀机制

学术界普遍认为早期地球开放大洋储库存在微摩尔级浓度(<100μmol)的 Fe^{2+}(Holland, 1973, 1984),海洋中存在大量 Fe^{2+} 的状态大约持续到 1.8Ga(Holland, 1984; Poulton et al. , 2004; Slack et al. ,2007),依据如下:① 大气圈与水圈为还原环境,处于低氧化水平(Holland, 1984; Bekker et al. , 2004);② 海洋硫酸盐及硫化物浓度很低(Canfield and Teske, 1996; Habicht et al. ,2002);③ 海底热液带来丰富的 Fe(Kump and Seyfried, 2005)。早在 20 世纪 70 ~ 80 年代,就有学者发现 BIFs 中磁铁矿交代早期赤铁矿与菱铁矿的现象(Ayres, 1972; Ewers and Morris, 1981)。地质学家认为,BIFs 沉淀的原始矿物为水铁矿 $Fe(OH)_3$,水铁矿经脱水作用可形成赤铁矿 Fe_2O_3,赤铁矿在后期成岩作用过程中被还原为磁铁矿 Fe_3O_4(Klein, 2005; Bekker et al. ,2010; Mloszewska et al. ,2012; Posth et al. ,2014)。因此,BIFs 沉淀的核心内容就是将 Fe^{2+} 氧化为 Fe^{3+},进而形成 $Fe(OH)_3$(Klein, 2005; Bekker et al. , 2010; Czaja et al. ,2013)。在长达一个多世纪的调查与争论之后,BIFs 的沉淀机制始终未能解决。BIFs 形成的时间跨度很大,其沉积环境从太古宙缺氧环境逐渐演变为古元古代部分氧化环境(Bekker and Kaufman, 2007),表明 BIFs 可能是通过不同的氧化机制形成(Bekker et al. ,2010)。

(1)生物产氧作用:Buick(1992)发现西澳大利亚 Tumbiana Formation 存在 2.7Ga 叠层石组合,其微生物席以蓝藻细菌为主;Eigenbrode and Freeman (2006)及 Eigenbrode 等(2008)指出 2.7Ga 页岩与碳酸盐岩中具有亏损 ^{13}C 的干酪根,暗示存在由蓝藻细菌及嗜甲烷菌组成的微生物群落;Buick(2008)还发现了含大量有机质的页岩;以上证据表明产氧光合作用(oxygenic photosynthesis) 在新太古代即已形成。Klein and Beukes(1989)认为原始大洋是层化的海洋:上部为较薄的氧化带,下部为含有大量 Fe^{2+} 的缺氧区域,二者之间为氧化还原变层(redoxcline)。上部氧化带为透光区域,发育大量蓝藻细菌并进行产氧光合作用。大陆风化来源的 Fe^{2+} 与深部海水上涌带来的 Fe^{2+} 在浅海氧化带汇合,经由以下反应形成 Fe^{3+}(Cloud, 1973):

$$2Fe^{2+} + 0.5O_2 + 5H_2O \longrightarrow 2Fe(OH)_3 + 4H^+ \quad (1)$$

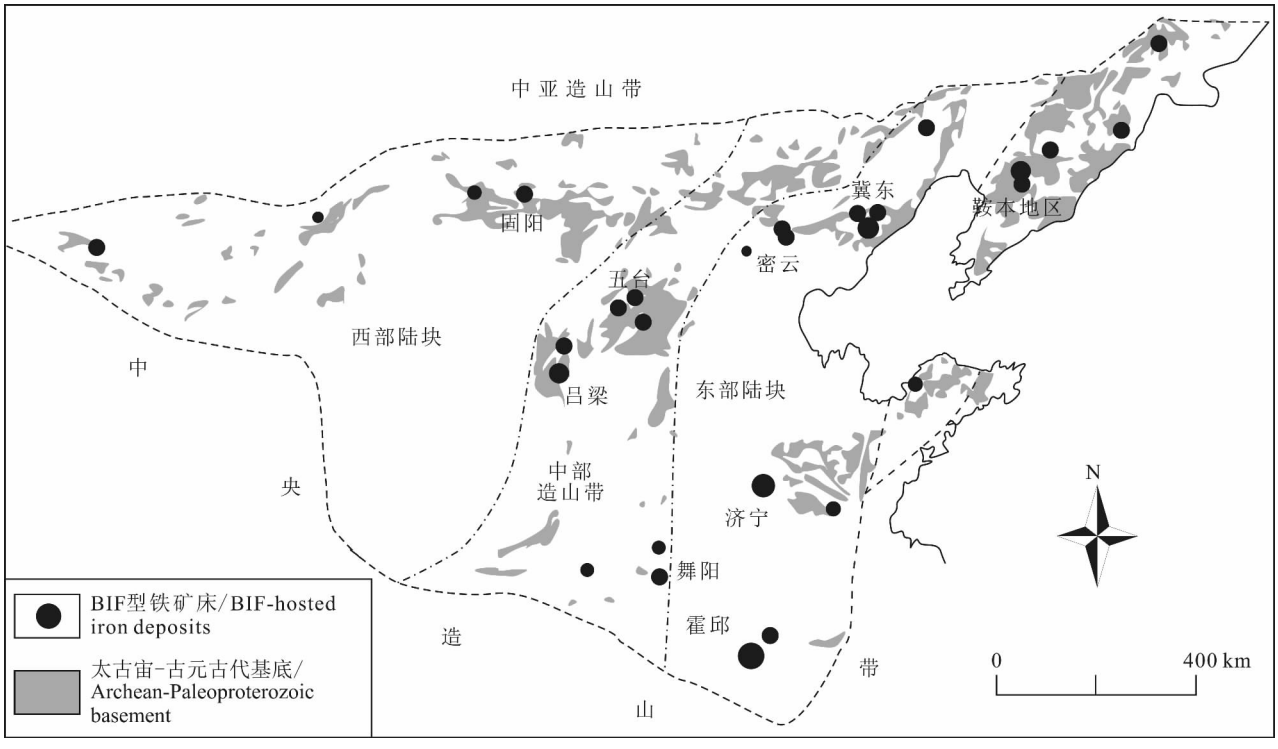

图 2 华北克拉通 BIFs 分布图(修改自 Zhao Guochun et al. ,2001;张连昌等,2012)

Fig. 2 The distribution of BIFs in the North China Craton (modified after Zhao Guochun et al. , 2001; Zhang Lianchang et al. , 2012)

(2)微生物新陈代谢:大约一个世纪以前,就有科学家发现在富 Fe 地下水中发育大量的嗜铁细菌(如 *Leptothrix* 与 *Gallionella*),并提出亲气微生物可能对 BIFs 沉积过程起了重要作用(Harder,1919)。近年来,科学家在实验室做了相关模拟实验,欲阐释微生物在 BIFs 形成中的重要性。他们发现亲气微生物能够利用 O_2、CO_2 及 H_2O 进行代谢反应(Bekker et al. ,2010):

$$6Fe^{2+} + 0.5O_2 + CO_2 + 16H_2O \longrightarrow [CH_2O] + 6Fe(OH)_3 + 12H^+ \quad (2)$$

这些亲气的 Fe^{2+} 氧化细菌被发现大量存在于在现代海洋系统中(Emerson and Moyer,2002)。Søgaard 等(2000)认为这些微生物具有很高的氧化效率,在低氧条件下能够主导 Fe 循环。Widdel 等(1993)发现某些细菌能够通过厌氧光合作用(anoxygenic photosynthesis),将 Fe^{2+} 作为电子供体生成 Fe^{3+}(Ehrenreich and Widdel, 1994):

$$4Fe^{2+} + 11H_2O + CO_2 \longrightarrow [CH_2O] + 4Fe(OH)_3 + 8H^+ \quad (3)$$

近 20 年来,大量实验表明各种紫色和绿色细菌能利用 Fe^{2+} 作为还原剂,从而固定 CO_2(Heising et al. , 1999;Straub et al. ,1999)。这些研究结果暗示在地质历史时期即使没有氧气,微生物也可以利用 Fe^{2+}、光及 CO_2 形成 BIFs(Bekker et al. ,2010)。

(3)紫外线光氧化作用:Cairns-Smith(1978)提出在大气圈氧气浓度升高及臭氧保护层形成之前,地球表层接受了大量紫外线光子的辐射,Fe^{2+} 能够被光氧化成为 Fe^{3+};该反应在酸性水体中、200 ~ 300 nm 波长的光照下能够稳步发生:

$$2Fe_{(aq)2+} + 2H^+ + h\nu(\text{紫外线光子辐射}) \longrightarrow 2Fe_{(aq)3+} + H_2 \quad (4)$$

Ohmoto 等(2004)认为多数 BIFs 主要由铁的碳酸盐及硅酸盐组成,暗示了非生物的海洋沉积成因。然而相关实验业已证实,Fe^{2+} 被光合自养细菌或氧气氧化为 Fe^{3+} 的效率远高于紫外线光氧化作用;BIFs 氧化物的前身是快速的、非光化学氧化过程的产物(Konhauser et al. ,2007)。因此,相比直接或间接的生物氧化作用,紫外线光氧化作用可能对 BIFs 沉积的贡献不是很大(Bekker et al. ,2010)。

(4)蒸汽与卤水相分离:Foustoukos and Bekker (2008)指出,一些深水相的 Algoma 型 BIFs 与 VMS 矿床紧密共生,前者可能是通过蒸汽与卤水相分离

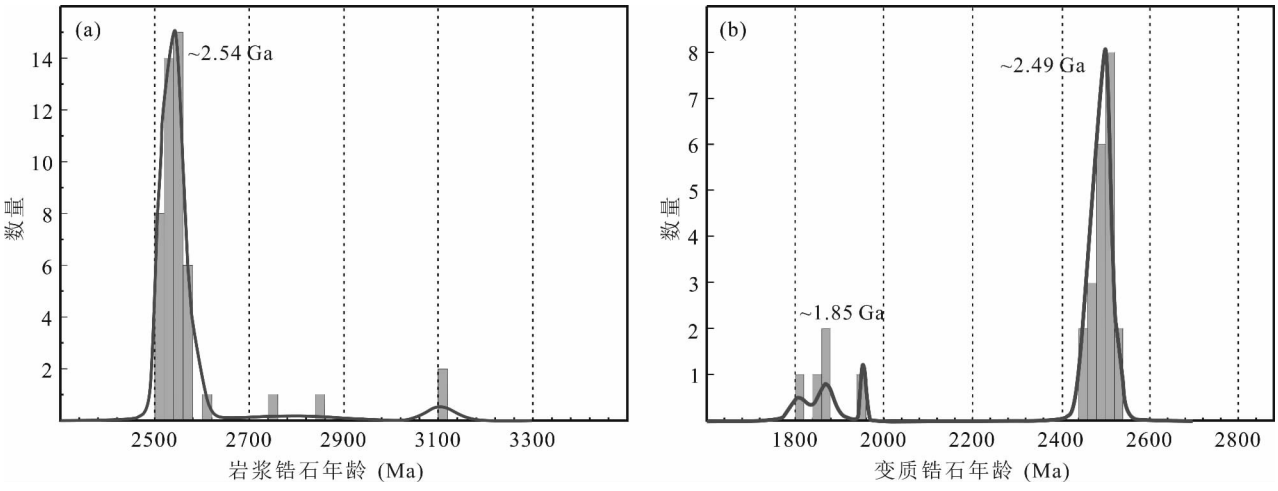

图 3 华北克拉通 BIF 相关岩系中岩浆(a)及变质(b)锆石 U-Pb 年龄统计图

Fig. 3 The statistical charts of U-Pb ages for magmatic (a) and metamorphic (b) zircons from BIF-associated rocks in the North China Craton

的氧化而成。在该过程中,H_2 与 HCl 进入蒸汽相,卤水中则残留氧化及碱性条件;过渡金属将形成含氯络合物,并在卤水中富集。Bekker 等(2010)认为该观点虽然缺乏模拟及数据支持,但能够解释深水缺氧环境下一些太古宙 BIFs 与 VMS 型矿床紧密共生的原因。

1.4 沉积环境

作为早期地球特殊环境的产物,BIFs 的沉积环境理所应当具备一些特定因素。Trendall(2009)在研究 Hamersley BIF 沉积条件的基础之上,提出了形成 BIFs 的几个必要条件:① 超过百万年的构造稳定性;② 水足够深,以避免外源碎屑的混入及海底扰动;③ 盆地形状便于富含 Fe^{2+} 的深部水体流通自如。在 2005 年《Economic Geology》100 周年纪念文集中,Clout and Simonson(2005)认为形成大型 BIFs 需要满足三个条件:① 大型海底热液供给系统;② 发育宽广大陆架;③ 存在成层海洋,蕴含大量 Fe^{2+} 的海水能够从海底热液系统运移至远处的沉积中心。前已述及,太古宙—古元古代(3.8 ~ 1.8Ga)海洋中存在大量 Fe^{2+}(Holland,1973,1984),这是 BIFs 形成的物质基础。要避免海水中的 Fe^{2+} 在运移过程中被氧化为 Fe^{3+},古海洋必定是整体处于缺氧环境(Cloud,1973)。基于 BIFs 的 Ce 异常判别及 Fe 同位素研究,这一认识已得到地质学家的广泛认可(Bau and Dulski,1996;Klein,2005;Bekker et al.,2010;Planavsky et al.,2012)。

(1) BIFs 缺乏负 Ce 异常:自然界中 Ce 一般呈稳定的 +3 价离子,在氧化条件下 Ce 被氧化为 +4 价,Ce^{+4} 溶解度更高,从而导致 REE 配分曲线中的 Ce 负异常。因此,根据 Ce 异常可以有效判断古海洋的氧化还原状态(Wright et al.,1987;Liu et al.,1988)。Bau and Dulski(1996)认为常规算法下 Ce 负异常的出现与 La 正异常有关,并建立了用 Ce/Ce^* 和 Pr/Pr^* 来判别真正 Ce 负异常的图解(图 1b)。该图解显示,太古宙及古元古代早期 BIFs 位于正 La 异常区域;大氧化事件之后(晚于 2.4Ga)的 BIFs 落点更加分散,涵盖正 La 及正 Ce 异常区域;几乎所有 BIFs 均未出现负 Ce 异常,暗示 BIFs 沉积时古海洋处于缺氧环境(Bau and Dulski,1996;Bekker et al.,2010)。Shields and Webb(2004)研究发现,元古宙以后的海水均呈现明显的负 Ce 异常,表明显生宙大洋处于氧化环境并最终导致了 BIFs 的绝灭(Canfield,1998;Huston and Logan,2004;Kump and Seyfried,2005;Fairchild and Kennedy,2007)。

(2)BIFs 富集重 Fe 同位素:已有的研究表明,Fe 同位素可以有效示踪地质历史时期海水的氧化还原状态(Dauphas and Rouxel,2006;Planavsky et al.,2009,2012;Steinhoefel et al.,2009;孙剑和朱祥坤,2015)。当海洋完全氧化时,海水中的 Fe 接近完全沉淀,即没有发生 Fe 同位素分馏,沉淀的 Fe^{3+} 氧化物的 Fe 同位素代表当时海水的 Fe 同位素信息。业已证实,海水 Fe 同位素的 $\delta^{56}Fe_{IRMM}$ 值为负值或接近于零(Johnson et al.,2008)。当海水中的 Fe 完全

氧化时,Fe^{3+}氧化物的 $\delta^{56}Fe_{IRMM}$值也在零附近;当海水还没有完全氧化时,海水中的 Fe 部分沉淀,生成 Fe^{3+}氧化物会发生 Fe 同位素分馏,并且相对于溶液中的 Fe^{2+},沉积物会呈现重同位素富集(Bullen et al.,2001; Balci et al.,2006; 李志红等,2012)。Planavsky 等(2012)统计了全球 24 个太古宙及元古宙 BIFs 的 Fe 同位素信息,发现 3.0 ~ 2.4Ga 的 BIFs 的 $\delta^{56}Fe_{IRMM}$值平均为 0.4‰,2.32 ~ 1.88Ga 的 BIFs 的 $\delta^{56}Fe_{IRMM}$值平均为 0‰,暗示 BIFs 沉积时海水中的 Fe 发生了部分而非完全氧化,表明当时的海洋处于低氧逸度状态。

全球 BIFs 的形成时代几乎连续分布于 3.8 ~ 1.8 Ga (Huston and Logan,2004;Klein,2005),暗示早前寒武纪时期海洋化学性质稳定、长期处于缺氧与富 Fe^{2+}环境(Cloud,1973;Holland,1973,1984)。Huston and Logan(2004)研究了 Fe—S—O 矿物在不同物理化学条件下的稳定性,发现 Fe^{2+}在高氧化、富硫环境的现代海水中溶解度非常低;要使 Fe^{2+}在海水中具有高溶解度以便被携带、运移,其周围海水必定是处于低硫状态。BIFs 沉淀过程需要将 Fe^{2+}氧化为 Fe^{3+}(Klein,2005;Bekker et al.,2010;Czaja et al.,2013),多数学者将之归因于微生物相关的氧化作用(Klein and Beukes,1989; Søgaard et al.,2000;Konhauser et al.,2002,2009;Kappler et al.,2005;Bekker et al.,2010)。本文指出,前寒武纪海洋处于整体缺氧、局部富氧(例如 BIFs 沉积的位置)的环境;富氧区域的氧气浓度足够使 Fe^{2+}发生氧化,却无法将 Ce^{3+}氧化 Ce^{4+},故 BIFs 不具备明显 Ce 负异常(Bau and Dulski,1996)。Klein(2005)认为 Fe^{2+}能够稳定存在于低氧逸度的酸性水体中,磁铁矿的形成则需要较高的氧逸度及中—碱性环境。近年来,相关实验结果业已证实嗜铁细菌的生存需要中—碱性环境(Konhauser et al.,2002;Kappler and Newman,2004;Kappler et al.,2005)。因此,BIFs 的沉淀可能是富 Fe^{2+}、处于低氧及低硫状态的酸性溶液在运移过程中遭遇环境突变(如氧气浓度升高、pH 值升高)的结果。

另外,Haugaard 等(2013)对比研究了西格陵兰 Itilliarsuk BIF(约 2.9 Ga)以及 Isua(约 3.8 Ga)与 Pongola(约 2.9 Ga)BIFs,发现随着 BIFs 形成年龄的减小,其 Eu/Eu * 值也会相应变小,并认为这是由于地球逐渐冷却导致热液活动变少的缘故(Condie,1997;Frei et al.,2008)。

1.5　条带成因

BIFs 的条带成因引起了众多地质学家的关注,包括原生沉积(条带为 S_0)及后期改造(条带为 S_1)两类观点。Bau and Dulski(1996)发现硅条带与铁条带具有不同的 Eu/Eu * 值,认为 BIFs 的互层条带为原生沉积成因。Seibold(1958)在考察 Adriatic 闭塞海湾富 Ca 及富 Fe 地层的层序变化时,认为微生物光合作用的周期性与营养、温度及光线等因素息息相关,可用于解释 BIFs 韵律层的成因。Cloud(1973)在阐释 BIFs 古生态学意义时,认为 Fe 为海底喷流成因,火山作用引起的热梯度能够使洋底富 Fe 海水上升;在 pH 介于 6.8 ~ 7.5 的环境中,Si 会保持连续沉积;当 Fe^{2+}及营养物质富足时,浅海区域的微生物光合作用生成大量氧气并使得 Fe^{2+}沉淀形成铁条带;当 Fe^{2+}及营养物质匮乏时,微生物光合作用衰竭,无法供应氧气以促进 BIFs 的形成。因此,Fe^{2+}的供应或微生物活动的周期性变化是形成 BIFs 条带的原因(Cloud,1973)。Rona and Scott(1993)指出海底热液活动具有周期性(episodic);据此,Ohmoto 等(2006)认为海底热液脉动式供给正是形成 BIFs 互层条带的主因,这一认识与上述 Cloud(1973)的观点类似。Drever(1974)认为季节变化会引起上升洋流强度的变化,后者可以解释硅铁韵律层成因:温暖气候条件下,上升洋流在浅海区域被快速氧化形成 Fe 条带,尔后持续的蒸发将会形成 Si 条带。Garrels(1987)研究二叠纪 Castile 蒸发岩(Anderson and Kirkland,1966)时,发现蒸发作用先使方解石结晶形成方解石条带,然后晶出硬石膏形成硬石膏条带;他认为该蒸发岩中的条带状构造与 BIFs 硅铁韵律条带非常相似,由此提出可以用蒸发作用对 BIFs 条带成因加以解释。Krapež 等(2003)对西澳大利亚古元古代 Brockman BIF 进行了详细的层序地层学研究,发现砂岩、泥岩、灰岩及 BIF 中均发育密度流(density current)韵律层,认为 BIFs 硅铁条带由密度流沉积而成。Posth 等(2008)通过实验室研究及地球化学模拟发现,在 20 ~ 25℃时,由微生物氧化导致的 Fe^{3+}矿物沉淀量达到最大值;在 4℃左右时,Fe^{3+}矿物沉淀量极小而 Si 沉淀量达到最大值。因此,他们认为海水温度波动是形成硅铁条带互层的原因。Wang Yifei 等(2009)基于热力学计算,提出热液淋滤低 Al 洋壳岩石(如科马提岩)可以形成富 Fe 及 Si 的流体;流体上升与周围海水混合,经自组织化学振荡(self-organized chemical oscillations)分别沉淀出 Fe 与 Si 进而形成 BIFs 条

带。Rasmussen 等(2013)发现澳大利亚 Brockman 蚀变很少的 BIF 中常发育一种微球粒,主要为富铁硅酸盐(黑硬绿泥石)并构成了沉积纹层;他们认为 BIFs 条带是富铁硅酸盐间歇性沉淀的结果。Li Yiliang(2014)利用扫描及透射电子显微镜对三个典型的新太古代—古元古代 BIFs 进行了组构分析,认为赤铁矿纳米条带(17 ~ 26nm)反映了 Fe^{3+} 的昼夜沉淀,燧石/碧玉微条带(3 ~ 12μm)则代表了年度沉积,二者与 BIFs 沉积速率吻合。

James(1969)对比红海含铁沉积物、铁石(ironstone)及 BIFs 时指出,BIFs 的条带状构造可能是原生的铁硅酸盐矿物在后期埋藏条件下,经成岩及脱水过程中的化学分异作用所致。随后,Cloud(1973)否定了这种观点,认为太古宙 BIFs 各个层位均显示逐渐尖灭的特征,故互层的硅铁条带是一种原生构造。Katsuta 等(2012)研究加拿大 Bell Lake BIF(2.8Ga)时,发现角闪岩相变质面理切割硅铁条带,表明 BIF 条带形成于峰期变质作用之前,他们认为 BIF 条带为原始沉积纹层;X 射线荧光光谱分析显示 Fe 条带中存在变质分异作用:角闪石与磁铁矿发生次生富集加大,Mn 聚集于 Fe 条带边部,Ti 基本不发生迁移。Sun Zhilei 等(2013)对 Valu Fa 海岭热液喷口的 Fe—Ti 氧化物做了详细的矿物学研究,认为生物成因的 Fe 氧化物与海水中溶解的 Si 具有化学结合效应(binding effect),无法单独沉淀出来;继而提出太古宙海洋并不能沉淀出硅铁韵律层,后者应该是氧化条件下的后期成岩过程所致。

2 国内 BIF 研究进展和问题

中国的 BIFs 多数产自华北克拉通,主要分布于鞍山—本溪、冀东、鲁西、五台—吕梁、内蒙古固阳、河南舞阳及安徽霍邱等地(图 2)。在我国,对 BIFs 的系统研究始于上世纪 50 年代(程裕淇,1957)。半个多世纪以来,中国地质学家对国内 BIFs 特征总结如下:①多分布于华北克拉通边缘及裂谷之中;②围岩主要产于新太古代,其次为古元古代;③围岩以变火山岩为主,兼含少量变沉积岩,铁矿床多属于 Algoma 型;④后期复杂的变质变形作用对 BIFs 改造强烈;⑤以贫矿为主,富矿少且多位于深部(Zhai Mingguo et al., 1990; Zhai Mingguo and Windley, 1990; 沈保丰等, 2006; 万渝生等, 2012; Zhang Lianchang et al.,2012; Li Houmin et al.,2014)。

2.1 主要研究进展

随着实验测试技术的不断发展,国内学者在前人研究基础之上对华北克拉通 BIFs 有了更深入的认识,主要包括年代学研究、物质来源及矿床成因等方面。

2.1.1 年代学研究

华北克拉通绝大多数 BIFs 与火山活动关系密切,属于 Algoma 型(沈保丰等,2006;万渝生等,2012;Zhang Lianchang et al.,2012;Li Houmin et al.,2014)。因此,BIFs 与变火山岩夹层或围岩是同一期火山—沉积作用的产物,变火山岩年龄可以间接代表 BIFs 形成时代(Trendall et al.,1998;Zhang Xiaojing et al.,2011;Cabral et al.,2012;Zhang Lianchang et al.,2012)。近年来,国内学者对华北克拉通 BIF 相关岩系做了大量锆石 U-Pb 年代学研究,本文从中挑选了可信度较高的年龄数据列于表 1。统计表明,这些 BIFs 多形成于约 2.54Ga(图 3a),并经历了新太古代晚期和古元古代晚期两期变质作用(图 3b);这一认识目前已被学者广泛认可(沈保丰等,2006;Zhang Xiaojing et al.,2011;万渝生等,2012;Zhang Lianchang et al.,2012)。

2.1.2 古海洋环境及物质来源

中国学者同样发现华北克拉通太古宙 Algoma 型 BIFs 明显缺乏 Ce 负异常并富集 Fe 重同位素,认为当时的海洋整体处于缺氧环境;稀土元素示踪表明,BIF 沉积作用与海底高温热液具有成因联系(李志红等,2008,2012;沈其韩等,2009,2011;Zhang Xiaojing et al.,2011;代堰锫等,2012,2013;蓝廷广等,2012;刘利等,2012;Dai Yanpei et al.,2014;Lan Tingguang et al.,2014a,2014b;Ma Xudong et al.,2014;Sun Xiaohui et al.,2014a)。王长乐等(2014)对山西吕梁古元古代袁家村 BIF(2.3 ~ 2.1Ga)进行了详细的稀土元素分析,显示部分 Ce 正异常、较小的 Y/Ho 比值(平均 30.89)与较低的 $(Ni/Fe)_{mol}$ 值(2.1×10^{-4} ~ 1.4×10^{-4});他们认为大氧化事件对海洋的化学成分产生了重要影响,说明 2.3 ~ 2.1Ga 古海洋是氧化还原状态分层的水体(王长乐等,2014)。

此外,李志红等(2008)发现鞍本地区 BIFs 的 $\delta^{57}Fe_{IRMM}$ 值与 Eu 异常大小呈正比,认为这一结果从成矿元素本身为 Fe 来源于海底火山热液活动提供了直接证据。李厚民等(2012)在弓长岭二矿区识别出一套与 BIF 整合产出的白云质大理岩,其 $\delta^{13}C_{V-PDB}$ 值为 -6.0‰ ~ -7.0‰,与地幔值一致;^{13}C 亏损的特征暗示大理岩为海底喷气沉积成因,亦表明该 BIF 的发育与海底热液活动有关。蒋少涌等

(1992)发现鞍本地区弓长岭 BIF 强烈亏损^{30}Si($\delta^{30}Si_{NBS-28}$ = -2.2‰ ~ -0.9‰);Hou Kejun 等(2014)获得山西袁家村 BIF 的$\delta^{30}Si_{NBS-28}$值介于-1.7‰ ~ -0.4‰,平均-1.1‰;李延河等(2010)及 Li Yanhe 等(2014)统计了华北克拉通不同时代、不同类型 BIFs 的硅同位素组成,$\delta^{30}Si_{NBS-28}$值介于-2.0‰ ~ -0.3‰,平均-0.8‰;以上 Si 同位素分析结果暗示华北克拉通 BIFs 中的 Si 属热液成因。

2.1.3　构造环境及矿床成因

目前,多数国内学者认为华北克拉通太古宙 Algoma 型 BIFs 产于俯冲相关构造背景。例如,Zhang Xiaojing 等(2011)认为冀东水厂 BIF(2547Ma)与斜长角闪片麻岩夹层形成于同一时代,后者具有贫 Ti、富轻稀土及大离子亲石元素、亏损重稀土及高场强元素特征,据此提出该 BIF 形成于岛弧或者弧后盆地环境。学者对其他 BIFs 的研究也提出了相同认识,如冀东石人沟 BIF(Zhang Lianchang et al.,2012)、鞍本齐大山 BIF(Sun Xiaohui et al.,2014b)、陈台沟 BIF(代堰锫等,2013)、弓长岭 BIF(Sun Xiaohui et al.,2014a,2014b)、歪头山 BIF(代堰锫等,2012)等。刘利等(2012)发现固阳地区三合明 BIF(2562Ma)斜长角闪岩围岩具有 T-MORB 特征,结合区内岩石组合特征及前人提出的岛弧叠加地幔柱模式(陈亮,2007),认为该 BIF 形成于弧后盆地并有地幔柱叠加的构造环境。Ma Xudong 等(2014)在研究固阳地区东五分子 BIF(2538Ma)时,认为东五分子绿岩带形成于太古宙板块俯冲过程;基于区内两种科马提岩的发育,提出该 BIF 的形成与洋中脊俯冲导致板片窗地幔上涌有关。

Superior 型 BIF 在华北克拉通发育较少,以袁家村 BIF(王长乐等,2014,2015;Wang Changle et al.,2015)以及霍邱 BIF(Yang Xiaoyong et al.,2014;Liu Lei and Yang Xiaoyong,2015)较为典型。王长乐等(2015)依据原生矿物的共生组合及产出特征,将袁家村 BIF 沉积相划分为氧化物相(60%)、硅酸盐相(30%)和碳酸盐相(10%)。Wang Changle 等(2015)对该 BIF 围岩(袁家村组变沉积岩)进行了地球化学研究,K_2O/Na_2O—SiO_2、SiO_2/Al_2O_3—K_2O/Na_2O 以及 Th—Co—Zr 图解均显示变沉积岩形成于被动大陆边缘环境。袁家村组地层中不发育同沉积火山岩(Zhao Guochun et al.,2008),与火山弧背景或大陆裂谷环境明显不同,进一步表明袁家村 BIF 沉积于被动大陆边缘,很可能是稳定的大陆架环境(Wang Changle et al.,2015)。霍邱 BIF 自下而上可分为两个矿带:下部为变粒岩—片岩—磁铁石英岩建造,上部为片岩—大理岩—赤铁(镜)石英岩建造(杨晓勇等,2012)。Yang Xiaoyong 等(2014)认为霍邱地区角闪岩与变基性岩的地球化学特征与弧后盆地火山岩类似,提出霍邱 BIF 形成于弧后盆地环境。Liu Lei and Yang Xiaoyong(2015)指出霍邱 BIF 之中不发育火山岩夹层,围岩斜长角闪岩与片麻岩形成于大陆弧或岛弧背景,且 BIF 与围岩的锆石年龄谱有很好的对应关系,认为霍邱 BIF 沉积于大陆边缘海或弧后盆地背景。

此外,蓝廷广等(2012)及 Lan Tingguang 等(2014a,2014b)发现鲁东昌邑 BIF(2240 ~ 2193Ma)沉积过程中有大量陆源碎屑物质的参与,围岩中含有较多酸性到中—基性火山岩,总体上显示双峰式特征,指出该 BIF 形成于大陆裂谷环境。李延河等(2010,2012)对比了 Algoma 与 Superior 型 BIFs 的 Si、O、Fe 同位素特征,认为两种类型 BIFs 均由地球早期的海底热液喷气作用在大气氧浓度不足现在大气氧水平 1% 的还原条件下形成,二者属于同一成矿系统;Algoma 型 BIF 距离同期火山活动中心更近,形成时代稍早,多形成于环境更加还原的深水盆地,而 Superior 型 BIF 与之恰好相反。

2.2　存在问题

相对于国外典型 BIFs,华北克拉通 BIFs 明显遭受了后期变质—变形作用的强烈叠加改造,为研究工作增加了难度。在我国,对 BIFs 的研究几近停顿了 30 年左右。由于时代的局限,前人工作缺乏对现代先进测试技术的应用。因此,国内 BIF 相关领域(特别是在 BIF 成矿的根本性问题上)的研究程度落后于国际舞台,亦存在诸多不足。

2.2.1　BIF 类型不清

Gross(1980,1983,1996)基于 BIFs 形成时代、赋矿建造及产出构造背景,将之划分为 Algoma 型及 Superior 型;前者含矿建造多为变火山岩,后者则以变沉积岩为主。国内学者往往根据赋矿岩系的原岩建造特征来划分 BIF 类型。例如,侯可军等(2007)认为,东西鞍山的变质岩石组合以绢云千枚岩 + 黑云母变粒岩 + 云母石英片岩夹斜长角闪岩 + 铁英岩为主,原岩建造为泥质 + 中酸性杂砂(夹基性火山岩) + 硅铁质沉积,远离火山活动中心,火山物质的含量相对较少,属 Superior 型或 Algoma—Superior 之间的过渡类型。实际上,国外一些典型绿岩带的上部沉积岩组合中同样发育 BIFs,如著名的南非

表 1 华北克拉通 BIF 相关岩系锆石 U-Pb 年龄统计表

Table 1 The statistics of zircon U-Pb ages for BIF-associated rocks in the North China Craton

区域	地点	岩群	岩性	产状	测年方法	锆石年龄 (Ma)			资料来源
						碎屑锆石	岩浆锆石	变质锆石	
辽宁鞍本	大孤山	鞍山岩群	绿泥石英片岩	BIF 夹层	A		3110±32		Dai Yanpei et al., 2014
				BIF 围岩	B		3101±28		
	陈台沟			BIF 夹层		2739±50	2551±10	2469±23	代堰锫等, 2013
	南芬		绿泥角闪片岩	BIF 夹层		2617±36	2554±14	2484±12	Zhu Mingtian et al., 2015
			磁铁石英岩					2480±63	
	歪头山		斜长角闪岩	BIF 夹层	A	2610±5	2533±11		代堰锫等, 2012
	东鞍山		黑云绿泥石英片岩	BIF 夹层	C		2544±8		杨秀清, 2013
	齐大山		黑云变粒岩	BIF 围岩	D		2533±53		王守伦和张瑞华, 1995
			正长花岗岩	侵入 BIF	C		2503±10		Wan Yusheng et al., 2012a
			黑云绿泥石英片岩	BIF 夹层			2530±6		杨秀清, 2013
	弓长岭		角闪变粒岩	BIF 围岩		~2700	2528±10		万渝生等, 2012
			斜长角闪片岩	BIF 围岩			2554±12		Han Chunming et al., 2014b
			蚀变石榴子石岩					1861±25	刘明军, 2013
辽北清原	小莱河	清原岩群	角闪变粒岩	BIF 夹层			2515±6		万渝生等, 2005
辽西建平	安太沟村口	建平岩群	磁铁石英岩		D			2488±1; 1806±16	王长秋等, 1999
					C		2520±11; 2552±13	2487±2	
	西官营子		角闪斜长片麻岩	BIF 围岩	B		2555±7	2512±12	Liu Shuwen et al., 2011
鲁西地区	沂水蔡峪岩体	沂水岩群	英云闪长岩	包裹 BIF	C		2562±14	2518±13	沈其韩等, 2004
	济宁	济宁岩群	变酸性火山岩	BIF 围岩			2522±7		万渝生等, 2012
			变长英质火山岩	BIF 围岩			2561±15		王伟等, 2010
	杨庄	泰山岩群	斜长角闪岩	BIF 围岩	B		2615±61		赖小东和杨晓勇, 2012
	枣庄		黑云变粒岩	BIF 围岩	C	2699; 2572			Wan Yusheng et al., 2012b
	韩旺		黑云变粒岩	BIF 围岩		2520			
胶东地区	固山水库	胶东岩群	角闪变粒岩	BIF 围岩			2519	2447±6	万渝生等, 2012
	马兰庄		花岗片麻岩	顺层侵入 BIF				2484±23	李延河等, 2011
	王寺峪		黑云斜长片麻岩	BIF 围岩	B		2516±9		曲军峰等, 2013
	石人沟		斜长角闪岩	BIF 夹层	A		2553±31	2510±21	Zhang Lianchang et al., 2012
			角闪斜长片麻岩	BIF 围岩			2541±21	2512±13	

				A				
	水厂	迁西岩群	斜长角闪片麻岩	BIF 夹层		2547±7	2513±4	Zhang Xiaojing et al., 2011
	棒磨山		混合岩	BIF 围岩	C		2523±13	2511±18	Li Lixing et al., 2015
	马兰庄		变粒岩	BIF 围岩			2545±16	2500±17	
	神龙峡		花岗片麻岩	BIF 围岩			2526±26	2528±17	
冀东地区	豆子沟		混合岩	BIF 围岩			2529±27	2485±23	
			含磁铁矿正长岩	BIF 围岩			2577±29		
	司家营	滦县岩群	片麻状花岗闪长岩	BIF 围岩	A		2535±8		Cui Minli et al., 2014
			黑云变粒岩	BIF 夹层			2537±13		
			黑云斜长片麻岩	BIF 下盘			2543±14		
	迁安		黑云变粒岩	BIF 围岩	C		2534±8		Nutman et al., 2011
	青龙	朱杖子岩群	花岗岩砾石	BIF 围岩?			2510±10		孙会一等, 2010
			黑云斜长片麻岩	BIF 围岩			2540±6		
			变酸性火山岩	BIF 围岩			2516±8		
			黑云斜长变粒岩	BIF 夹层			2572±8		陈靖等, 2015
		单塔子岩群	黑云变粒岩	BIF 围岩			2504±7		孙会一等, 2010
密云地区	四合堂东北	密云岩群	黑云斜长片麻岩	BIF 围岩			2542±17	2505±6; 2448±14	Shi Yuruo et al., 2012
内蒙古	固阳乌兰不浪	兴和岩群	麻粒岩	BIF 围岩			2545±7	2530~2477	Dong Xiaojie et al., 2012
	三合明	色尔腾山群	斜长角闪岩	BIF 夹层	A		2562±14		刘利等, 2012
	公益民		斜长角闪岩	BIF 夹层			2569±78		Liu Li et al., 2014
	大青山	乌拉山岩群	石榴黑云片麻岩	BIF 围岩	C	2572~2450		2467±7; 1954±5	董春艳等, 2012
山西五台	峨口	五台岩群	变安山岩	BIF 围岩			2529±10		Wilde et al.,2005
	王家庄		斜长角闪岩	BIF 围岩	A		2543±4		Wang Changle et al.,2014
山西吕梁	袁家村	吕梁岩群	变砂岩	BIF 围岩		2757~2348			Wang Changle et al.,2015
安徽霍邱	霍邱	霍邱岩群	斜长角闪岩	BIF 围岩	B		2846±82		杨晓勇等, 2012
			二长片麻岩	BIF 围岩			2752±75		Yang Xiaoyong et al., 2014
			石榴黑云角闪片麻岩	BIF 围岩	C	2982; 2739			万渝生等, 2012
			磁铁石英岩			2970; 2753			Liu Li and Yang Xiaoyong, 2015
河南鲁山	水滴沟组	上太华岩群	石墨石榴夕线片麻岩	BIF 围岩	C	2730~2505		1844±66	Wan Yusheng et al., 2006
			含石榴子石片麻状花岗岩	侵入太华岩群			2139±16	1871±14	
河南登封	老羊沟	登封岩群	二云二长石英片岩	BIF 围岩		2687~2614	2508±16; 2531±15		万渝生等, 2009

注：测年方法中A=锆石SIMS，B=锆石LA-ICP-MS，C=锆石SHRIMP，D=单颗粒锆石稀释法。

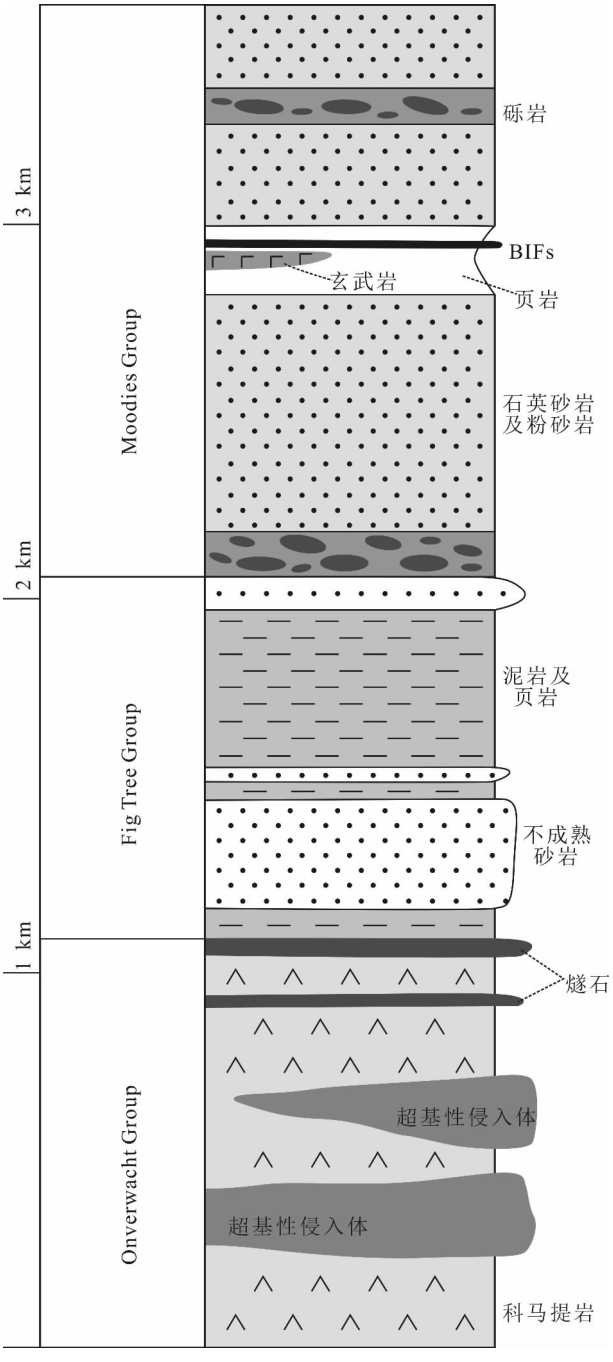

图 4 南非 Barberton 绿岩带地层柱状图(据 Bontognali et al. ,2013)

Fig. 4 The stratigraphic column of the Barberton greenstone belt, South African (Bontognali et al., 2013)

Barberton 绿岩带(图 4),但这些 BIFs 无疑当属 Algoma 型。因此在探讨 BIF 类型时,不能仅依据容矿围岩为变沉积岩就称之为 Superior 型;应结合地质构造背景,从地层柱发育序列进行综合判别(张连昌等, 2012)。

2.2.2 形成时代不准

前人对国内 BIF 相关岩系的年龄测定多采用 Sm-Nd 等时线法,该方法往往较实际年龄偏老(陆松年等,1995)。例如,乔广生等(1990)获得歪头山—北台硅铁建造中斜闪角长岩的全岩 Sm-Nd 年龄为 2724 ± 102 Ma,与其锆石 SIMS U-Pb 年龄相差甚远(2533 ± 11 Ma,代堰锫等,2012)。近年来高精度 U-Pb 定年技术的迅速发展,为精确厘定 BIF 型铁矿床的形成时代提供了契机。研究表明,锆石 U-Pb 法相对于 Sm-Nd 及 Re-Os 等时线法更为有效(Frei and Polat,2007;Ripley et al. ,2008);Algoma 型 BIF 变火山岩夹层或围岩的锆石 U-Pb 年龄可以间接代表 BIF 形成时代(Trendall et al., 1998; Zhang Xiaojing et al., 2011; Cabral et al., 2012; Zhang Lianchang et al. ,2012)。因此,本文对华北克拉通太古宙 BIF 相关岩系形成时代的统计,均采用可信度较高的锆石 U-Pb 年龄(表 1)。

相对而言,Superior 型 BIF 不含或含有极少量的火山岩(Gross,1980,1983,1996),获取其沉积时代难度较大。Wang Changle 等(2015)对袁家村 BIF 变沉积岩夹层进行了锆石 U-Pb 定年,最年轻一组碎屑锆石年龄为 2350Ma,代表了沉积时代下限;结合前人对上覆近周峪组变火山岩的定年结果(2213Ma,Liu Shuwen et al. ,2012),将该 BIF 形成年龄约束在 2350 ~ 2213Ma (Wang Changle et al., 2015)。Liu Lei and Yang Xiaoyong (2015) 对霍邱 BIF 铁矿石中挑选出的碎屑锆石进行了 U-Pb 定年,获得的最小一组锆石年龄为 2. 75Ga(不含 Pb 丢失锆石);此外,这些碎屑锆石年龄谱中缺失区域上发育的 2. 71Ga 或 2. 56Ga 岩浆事件记录,表明霍邱 BIF 形成于 2. 75 ~ 2. 71Ga 或 2. 75 ~ 2. 56Ga 之间(Liu Lei and Yang Xiaoyong,2015)。

2.2.3 缺乏古老 BIFs

前已述及,绝大多数华北克拉通 BIFs 均形成于约 2. 54Ga(图 3a);据报道仅有三例 BIFs 可能沉积于新太古代之前:冀东古太古代杏山 BIF(沈其韩,1998;沈保丰等,2006)、鞍山古太古代陈台沟 BIF(万渝生等,2012)及中太古代大孤山 BIF(Dai Yanpei et al. ,2014)。然而,杏山 BIF 的形成时代还存在较大争议:前人采用全岩 Sm-Nd 等时线法获得其沉积年龄为约 3. 5Ga(沈其韩,1998;沈保丰等,2006);Han Chunming 等(2014a)报道了围岩石榴子石斜长片麻岩 SHRIMP 锆石 U-Pb 定年结果,指出杏山 BIF 沉积于 3389. 5 ± 7. 6Ma;郑梦天等(2015)采

用 LA-ICP-MS 锆石 U-Pb 定年,发现铁矿体夹层斜长角闪岩原岩年龄介于 2859 ±22Ma 至 2491 ±13Ma 之间,认为杏山 BIF 形成时代最有可能为新太古代晚期。此外,陈台沟表壳岩(约 3362Ma,SHRIMP U-Pb 法,Song Biao et al. ,1996)中发育的 BIFs 规模不大且磁铁矿含量很低,按严格定义不能称之为 BIF(万渝生等,2012)。Dai Yanpei 等(2014)对鞍本地区大孤山 BIF 围岩进行了 SIMS 及 LA-ICP-MS 锆石 U-Pb 定年,认为绿泥石英片岩(BIF 夹层)形成于 3110 ~3101Ma、混合片麻岩(包裹 BIF 与片岩)形成于 2997 ~2995Ma,表明该 BIF 可能沉积于中元古代(约 3. 1Ga),与其较古老的 Sm-Nd 等时线年龄一致(3168 ±50Ma,代堰锫,2014)。全球最老的 BIFs 形成于 3. 8 ~3. 7Ga,如西格陵兰 Isua BIF(Dymek and Klein,1988)及加拿大魁北克省 Nuvvuagittuq BIF(Mloszewska et al. ,2012)。科学家对这些古老 BIFs 及相关岩系进行了系统研究,并从中提取出了诸多重要信息,如 3. 7Ga 前的海洋中已蕴含早期生命(Ohtomo et al. ,2014)、板块俯冲至少始于 3. 8Ga(Jenner et al. ,2009)。因此,对古老 BIFs 的精确厘定与深入研究有助于认识华北克拉通早期形成演化过程。

2.2.4　富矿成因不明

BIFs 中常局部发育富铁矿体(BIF-hosted high-grade iron orebodies),后者具有高的 Fe 含量(TFe > 50%,Li Houmin et al. ,2014)。长期以来,国内学者对富铁矿的成因众说纷纭、莫衷一是。究其原因,多是受限于我国富铁矿产出地质背景的复杂性,以及各家观点的局限性。

(1)风化淋滤:早在 100 多年前,已有学者针对国外 BIF 型富铁矿提出“风化淋滤”的观点(Leith,1903)并被沿用至今(Morris,1983,1985,1998;Clout,2003;Angerer and Hagemann,2010;Duuring and Hagemann,2013),意即 BIFs 在后期地质演化过程中遭受表生氧化和风化淋滤作用,其中的磁铁矿被氧化成假像赤铁矿、石英被淋滤出来,形成氧化富铁矿石。然而,该类富铁矿在我国发育甚少,仅见于庙儿沟、西鞍山等地(程裕淇,1957)。

(2)菱铁矿分解:李绍柄(1979)在研究弓长岭铁矿时,首次发现富铁矿石中有石墨的存在。基于矿床地质、矿石物质成分和结构构造的研究,他们提出弓长岭含石墨的富磁铁矿矿床是产于前寒武含铁岩系中的菱铁矿矿层;经后期区域变质作用影响,菱铁矿可能按如下反应转变成为石墨和磁铁矿组合:$6FeCO_3 \longrightarrow 2Fe_3O_4 + C + 5CO_2$。李曙光等(1983)研究了弓长岭石墨 C 同位素组成,发现两种成因类型的石墨,平均 $\delta^{13}C_{V-PDB}$ 值分别为 -26. 6‰ ± 0. 6‰以及 -4. 7‰ ± 1. 9‰;他们认为在早前寒武纪该区水圈中已有生命活动,并且形成石墨的原始碳酸盐可能是菱铁矿,后者在强还原条件下经变质分解形成石墨及磁铁矿。“菱铁矿分解成因”的观点近来被 O 同位素证据否定,刘军和靳淑韵(2010)认为沉积型菱铁矿 $\delta^{18}O_{V-SMOW}$ 值较高,如西澳大利亚 Hamersley BIF 中菱铁矿 $\delta^{18}O_{V-SMOW}$ 值平均为 20. 67‰(Becker and Clayton,1976);由菱铁矿分解形成的磁铁矿即使经变质作用后,也会保留有高的 $\delta^{18}O_{V-SMOW}$ 值,但他们分析的弓长岭磁铁富矿的 $\delta^{18}O_{V-SMOW}$ 值几乎全是负值,不具有菱铁矿变质形成的 O 同位素组成特点。

(3)原始沉积:陈光远等(1984)详细对比了贫富矿体的野外产状及成因矿物学特征,发现二者存在诸多相似之处,由此认为富铁矿层属原生沉积成因;野外可见磁铁石英岩角砾被富矿包裹,因此热液形成富矿的作用是次要的。万渝生(1993)发现富矿石粒度存在细粒及粗粒两种类型,二者在空间上相互伴生,矿物粒度亦相互过渡;认为细粒富矿主要为原生沉积变质成因,粗粒富矿是高温热液对细粒富矿作用的结果。然而,富矿石与 BIFs 组构明显不同,当中的磁铁矿成分存在较大差异,且富矿石 ΣREY、Eu/Eu *、$\delta^{57}Fe_{IRMM}$、$\delta^{18}O_{V-SMOW}$ 值相对偏低(代堰锫, 2014),表明二者并非形成于相同条件(Nold et al. ,2013)。据此本文认为,富矿体并非原始沉积成因,其形成过程可能受更为复杂或更为强烈的地质作用控制,应当是 BIFs 被后期地质作用改造的结果。

(4)岩浆热液:程裕淇(1957)详细论述了辽宁、山东等地区 BIFs 中富矿的成因问题,指出富矿体以热液交代型为主,热液活动往往与邻近的花岗质岩石或由花岗岩化(即混合岩化作用)生成的混合岩有关;热液中铁质来源与岩浆活动有关,也与花岗岩化作用有着一定联系。近来,Li Houmin 等(2015)研究了鞍本地区 BIFs 与富铁矿的 O、S 同位素组成,认为弓长岭富矿与中碱性大气降水热液导致的去硅作用有关,蚀变类型主要包括石榴子石化、阳起石化与绿泥石化;其他矿区(例如齐大山)富铁矿体则形成于中酸性混合岩化热液导致的铁质活化—再沉淀过程,蚀变类型主要为黑云母化和绿泥石化,该类型的富矿体发育较少可能是由于有限的混合岩化热液

(Li Houmin et al. ,2015)。

(5)变质热液:关广岳(1961)认为在鞍山式铁矿床中富矿体的形成主要与区域变质作用有关:区域变质过程中从围岩(包括 BIFs)挤压出来大量富含铁质的变质水,交代 BIFs 形成富矿体;磁铁富矿体周围发育的热液蚀变岩中的主要矿物,如石榴子石、绿泥石及镁铁闪石等,实际上是典型的区域变质矿物。这一论点受到了周世泰(1994)的支持,后者进一步指出变质热液温度在 350℃以上,且具有低 $\delta^{18}O_{V-SMOW}$ 特点;富矿石中的石英包裹体内未见磁铁矿子晶,表明成矿热液没有另外带来铁质(周世泰,1994)。

(6)构造富集:周永贵等(2012)发现冀东地区杏山 BIF 的石英磁铁矿层存在强烈塑性变形;他们认为在一定温压条件下磁铁矿能发生定向塑性流动,并运移至褶皱核部富集、重结晶后进而形成富大铁矿体。然而,前寒武纪 BIFs 动辄绵延几十千米,该理论似乎难以解释如此大尺度铁矿的富集机制。此外,磁铁矿塑性变形温度高于 600℃(Housen et al. ,1995;Mamtani et al. ,2011),冀东、鞍本等地区的变形条件(最高约 500℃)几乎不可能使磁铁矿发生塑性流动(代堰锫,2014)。

3 结语

前寒武纪 BIFs 蕴含丰富的铁矿石资源,记录了早期地球演化的重要信息,故而引起地质学家的极大兴趣。近年来,BIF 相关领域的研究取得了长足进展,国际学者普遍认为:① BIF 沉积过程与地幔柱、地壳增生等全球性重大地质事件相关;② Fe 来源于海水与海底高温热液的混合溶液,其中高温热液与海水比例约为 1:1000;③ BIFs 沉积时古海洋整体处于缺氧环境。此外,学者对一些关键问题存在较大争议,例如 Si 的主要来源(海底高温热液或是陆源风化产物)、BIFs 的沉淀机制及条带成因等。

华北克拉通 BIFs 多形成于约 2.54Ga,国内学者对其研究程度还略显不足。一些 BIFs 的类型判别存在误区,形成时代尚需精确厘定,古老 BIFs 与富矿成因有待进一步查明。本文认为,在翔实的野外地质调查基础之上,应用现代先进测试技术(如高精度锆石 U-Pb 定年及 Fe—Si—Nd 同位素分析等)、加强与国外典型 BIFs 的对比研究,无疑对探索 BIF 沉积事件的精细过程及华北克拉通的早期演化历史大有裨益。

致谢:万渝生研究员和另一位审稿专家为本文的修改和完善提供了诸多有益建议,作者表示由衷感谢!

参 考 文 献 / References

(The literature whose publishing year followed by a "&" is in Chinese with English abstract; the literature whose publishing year followed by a "#" is in Chinese without English abstract)

陈光远, 黎美华, 汪雪芳. 1984. 弓长岭铁矿成因矿物学专辑. 矿物岩石, 4(2): 74 ~ 109.

陈靖, 李厚民, 罗迪柯, 李立兴, 杨秀清, 刘明军, 姚通, 胡彬. 2015. 冀东柞栏杖子 BIF 地球化学特征、形成时代及其地质意义. 地质通报, 34(5): 919 ~ 929.

陈亮. 2007. 固阳绿岩带的地球化学和年代学. 导师: 郭敬辉, 翟明国. 北京: 中国科学院地质与地球物理研究所博士后出站报告, 1 ~ 40.

程裕淇. 1957. 中国东北部辽宁山东等省前震旦纪鞍山式条带状铁矿中富矿的成因问题. 地质学报, 37(2): 153 ~ 189.

代堰锫, 张连昌, 王长乐, 刘利, 崔敏利, 朱明田, 相鹏. 2012. 辽宁本溪歪头山条带状铁矿的成因类型、形成时代及构造背景. 岩石学报, 28(11): 3574 ~ 3594.

代堰锫, 张连昌, 朱明田, 王长乐, 刘利. 2013. 鞍山陈台沟 BIF 铁矿与太古代地壳增生: 锆石 U-Pb 年龄与 Hf 同位素约束. 岩石学报, 29(7): 2537 ~ 2550.

代堰锫. 2014. 鞍本地区太古宙两期 BIF 成矿作用及富矿成因. 导师: 张连昌. 北京: 中国科学院地质与地球物理研究所博士学位论文, 1 ~ 166.

董春艳, 万渝生, 徐仲元, 刘敦一, 杨振升, 马铭株, 颉颃强. 2012. 华北克拉通大青山地区古元古代晚期孔兹岩系: 锆石 SHRIMP U-Pb 定年. 中国科学: 地球科学, 42(12): 1851 ~ 1862.

关广岳. 1961. 论变质作用在鞍山式铁矿床富矿形成上的意义. 地质学报, 41(1): 65 ~ 76.

侯可军, 李延河, 万德芳. 2007. 鞍山—本溪地区条带状硅铁建造的硫同位素非质量分馏对太古代大气氧水平和硫循环的制约. 中国科学 D 辑: 地球科学, 37(8): 997 ~ 1003.

蒋少涌, 丁悌平, 万德芳, 李延河. 1992. 辽宁弓长岭太古代条带状硅铁建造(BIF)的硅同位素组成特征. 中国科学 B 辑, (6): 626 ~ 631.

赖小东, 杨晓勇. 2012. 鲁西杨庄条带状铁建造特征及锆石年代学研究. 岩石学报, 28(11): 3612 ~ 3622.

蓝廷广, 范宏瑞, 胡芳芳, 杨奎锋, 郑小礼, 张华东. 2012. 鲁东昌邑古元古代 BIF 铁矿矿床地球化学特征及矿床成因讨论. 岩石学报, 28(11): 3595 ~ 3611.

李厚民, 刘明军, 李立兴, 杨秀清, 陈靖, 姚良德, 洪学宽, 姚通. 2012. 辽宁弓长岭铁矿区大理岩地质地球化学特征及其成矿意义. 岩石学报, 28(11): 3497 ~ 3512.

李绍柄, 1979. 我国铁矿床的一种新类型——弓长岭式含石墨的富磁铁矿矿床及其成因. 地球化学, (2): 170 ~ 177.

李曙光, 支霞臣, 陈江峰, 王俊新, 邓衍尧. 1983. 鞍山前寒武纪条带状含铁建造中石墨的成因. 地球化学, (2): 162 ~ 169.

李延河, 侯可军, 万德芳, 张增杰, 乐国良. 2010. 前寒武纪条带状硅铁建造的形成机制与地球早期的大气和海洋. 地质学报, 84(9): 1359 ~ 1373.

李延河, 张增杰, 伍家善, 尚龙平. 2011. 冀东马兰庄条带状硅铁建造的变质时代及地质意义. 矿床地质, 30(4): 645 ~ 653.

李延河, 侯可军, 万德芳, 张增杰. 2012. Algoma 型和 Superior 型硅铁建造地球化学对比研究. 岩石学报, 28(11): 3513 ~ 3519.

李志红, 朱祥坤, 唐索寒. 2008. 鞍山—本溪地区条带状铁建造的铁同位素与稀土元素特征及其对成矿物质来源的指示. 岩石矿物学杂志, 27(4): 285 ~ 290.

李志红, 朱祥坤, 唐索寒, 2012. 鞍山—本溪地区条带状铁矿的 Fe 同位素特征及其对成矿机理和地球早期海洋环境的制约. 岩石学报, 28(11): 3545 ~ 3558.

刘军, 靳淑韵. 2010. 辽宁弓长岭铁矿磁铁富矿的成因研究. 现代地质, 24(1): 80 ~ 88.

刘利, 张连昌, 代堰锫, 王长乐, 李智泉. 2012. 内蒙古固阳绿岩带三合明 BIF 型铁矿的形成时代、地球化学特征及地质意义. 岩石学报, 28(11): 3623 ~ 3637.

刘明军, 2013. 辽宁弓长岭沉积变质型铁矿热液改造作用及其成矿意义. 导师: 薛春纪, 李厚民. 北京: 中国地质大学 (北京) 硕士学位论文, 1 ~ 113.

陆松年, 杨春亮, 李怀坤, 蒋明媚, 陈安蜀, 胡正德. 1995. 华北地台前寒武纪变质基底的 Sm-Nd 同位素地质信息. 华北地质矿产杂志, 10(2): 143 ~ 153.

乔广生, 翟明国, 阎月华. 1990. 鞍山地区太古代岩石同位素地质年代学研究. 地质科学, 2(2): 158 ~ 164.

曲军峰, 李锦轶, 刘建峰. 2013. 冀东地区王寺峪条带状铁矿的形成时代及意义. 地质通报, 32(2 ~ 3): 260 ~ 266.

沈保丰, 翟安民, 陈文明, 杨春亮, 胡小蝶, 曹秀兰, 宫晓华. 2006. 中国前寒武纪成矿作用. 北京: 地质出版社, 1 ~ 362.

沈其韩. 1998. 华北地台早前寒武纪条带状铁英岩地质特征及形成的地质背景. 程裕淇, 华北地台早前寒武纪地质研究论文集. 北京: 地质出版社, 1 ~ 30.

沈其韩, 宋彪, 徐惠芬, 耿元生, 沈昆. 2004. 山东沂水太古宙蔡峪和大山岩体 SHRIMP 锆石年代学. 地质论评, 50(3): 275 ~ 284.

沈其韩, 宋会侠, 赵子然. 2009. 山东韩旺新太古代条带状铁矿的稀土和微量元素特征. 地球学报, 30(6): 693 ~ 699.

沈其韩, 宋会侠, 杨崇辉, 万渝生. 2011. 山西五台山和冀东迁安地区条带状铁矿的岩石化学特征及其地质意义. 岩石矿物学杂志, 30(2): 161 ~ 171.

孙会一, 董春艳, 颉颃强, 王伟, 马铭株, 刘敦一, Nutman A, 万渝生. 2010. 冀东青龙地区新太古代朱杖子群和单塔子群形成时代: 锆石 SHRIMP U-Pb 定年. 地质论评, 56(6): 888 ~ 898.

孙剑, 朱祥坤. 2015. 表生过程中铁的同位素地球化学. 地质论评, 61(6): 1370 ~ 1382.

万渝生. 1993. 辽宁弓长岭含铁岩系的形成与演化. 北京: 北京科学技术出版社, 1 ~ 99.

万渝生, 宋彪, 杨淳, 刘敦一. 2005. 辽宁抚顺—清原地区太古宙岩石 SHRIMP 锆石 U-Pb 年代学及其地质意义. 地质学报, 79(1): 78 ~ 87.

万渝生, 刘敦一, 王世炎, 赵逊, 董春艳, 周红英, 殷小艳, 杨长秀, 高林志. 2009. 登封地区早前寒武纪地壳演化——地球化学和锆石 SHRIMP U-Pb 年代学制约. 地质学报, 83(7): 982 ~ 999.

万渝生, 董春艳, 颉颃强, 王世进, 宋明春, 徐仲元, 王世炎, 周红英, 马铭株, 刘敦一. 2012. 华北克拉通早前寒武纪条带状铁建造形成时代——SHRIMP 锆石 U-Pb 定年. 地质学报, 86(9): 1447 ~ 1478.

王长乐, 张连昌, 兰彩云, 代堰锫. 2014. 山西吕梁古元古代袁家村铁矿 BIF 稀土元素地球化学及其对大氧化事件的指示. 中国科学: 地球科学, 44(11): 2389 ~ 2405.

王长乐, 张连昌, 兰彩云, 李红中, 黄华. 2015. 山西吕梁袁家村条带状铁建造沉积相与沉积环境分析. 岩石学报, 31(6): 1671 ~ 1693.

王长秋, 崔文元, Krner A, Nemchin A A. 1999. 辽西太古代建平变质杂岩中磁铁石英岩的锆石同位素年龄. 科学通报, 44(15): 1666 ~ 1670.

王守伦, 张瑞华. 1995. 齐大山铁矿黑云变粒岩单锆石年龄及意义. 矿床地质, 14(3): 216 ~ 219.

王伟, 王世进, 刘敦一, 李培远, 董春艳, 颉颃强, 马铭株, 万渝生. 2010. 鲁西新太古代济宁群含铁岩系形成时代——SHRIMP U-Pb 锆石定年. 岩石学报, 26(4): 1175 ~ 1181.

杨晓勇, 王波华, 杜贞保, 王启才, 王玉贤, 涂政标, 张文利, 孙卫东. 2012. 论华北克拉通南缘霍邱群变质作用、形成时代及霍邱 BIF 铁矿成矿机制. 岩石学报, 28(11): 3476 ~ 3496.

杨秀清, 2013. 辽宁鞍山—本溪变质岩区铁成矿过程研究. 导师: 薛春纪, 李厚民. 北京: 中国地质大学 (北京) 硕士学位论文, 1 ~ 136.

张连昌, 翟明国, 万渝生, 郭敬辉, 代堰锫, 王长乐, 刘利. 2012. 华北克拉通前寒武纪 BIF 铁矿研究: 进展与问题. 岩石学报, 28(11): 3431 ~ 3445.

郑梦天, 张连昌, 王长乐, 朱明田, 李智泉, 王亚婷. 2015. 冀东杏山 BIF 铁矿形成时代及成因探讨. 岩石学报, 31(6): 1636 ~ 1652.

周世泰. 1994. 鞍山—本溪地区条带状铁矿地质. 北京: 地质出版社, 1 ~ 277.

周永贵, 陈正乐, 陈柏林, 韩凤彬. 2012. 河北迁安杏山富大铁矿体成因初析. 吉林大学学报 (地球科学版), 42(S3): 81 ~ 92.

Alexander B W, Bau M, Andersson P, Dulski P. 2008. Continentally-derived solutes in shallow Archean seawater: Rare earth element and Nd isotope evidence in iron formation from the 2.9 Ga Pongola Supergroup, South Africa. Geochimica et Cosmochimica Acta, 72: 378 ~ 394.

Alibert C, McCulloch M T. 1993. Rare earth element and neodymium isotopic compositions of the banded iron-formations and associated shales from Hamersley, western Australia, Geochimica et Cosmochimica Acta, 57: 187 ~ 204.

Alibo D S, Nozaki Y. 1999. Rare earth elements in seawater: particle association, shale-normalization, and Ce oxidation. Geochimica et Cosmochimica Acta, 63: 363 ~ 372.

Anderson R Y, Kirkland D W, 1966. Intrabasin varve correlation. Geological Society of America Bulletin, 77: 241 ~ 256.

André L, Cardinal D, Alleman L Y, Moorbath S. 2006. Silicon isotopes in 3.8 Ga West Greenland rocks as clues to the Eoarchaean supracrustal silicon cycle. Earth and Planetary Science Letters, 245: 162 ~ 173.

Angerer T, Hagemann S G. 2010. The BIF-hosted high-grade iron ore deposits in the Archean Koolyanobbing Greenstone Belt, Western Australia: Structural control on synorogenic- and weathering-related magnetite-, hematite-, and goethite-rich iron ore. Economic Geology, 105(5): 917 ~ 945.

Ayres D E. 1972. Genesis of iron-bearing minerals in banded iron formation mesobands in the Dales Gorge Member, Hamersley Group, Western Australia. Economic Geology, 67: 1214 ~ 1233.

Balci N, Bullen T D, Witte-Lien K, Shanks W C, Motelica M, Mandernack K W. 2006. Iron isotope fractionation during microbially stimulated Fe(II) oxidation and Fe(III) precipitation. Geochimica et Cosmochimica Acta, 70: 622 ~ 639.

Barley M E, Pickard A L, Sylvester P J. 1997. Emplacement of a large igneous province as a possible cause of banded iron formation 2.45 billion years ago. Nature, 385: 55 ~ 58.

Barley M E, Bekker A, Krapežz B. 2005. Late Archean to Early Paleoproterozoic global tectonics, environmental change and the rise

of atmospheric oxygen. Earth and Planetary Science Letters, 238: 156 ~ 171.

Basta F F, Maurice A E, Fontbotéc L, Favargerd P Y. 2011. Petrology and geochemistry of the banded iron formation (BIF) of Wadi Karim and Um Anab, Eastern Desert, Egypt: Implications for the origin of Neoproterozoic BIF. Precambrian Research, 187: 277 ~ 292.

Bau M, Dulski P. 1996. Distribution of yttrium and rare-earth elements in the Penge and Kuruman iron formations, Transvaal Supergroup, South Africa. Precambrian Research, 79: 37 ~ 55.

Bau M, Hohndorf A, Dulski P, Beukes N J. 1997. Sources of rare-earth elements and iron in Palaeoproterozoic iron-formations from the Transvaal Supergroup, South Africa: Evidence from neodymium isotopes. The Journal of Geology, 105: 121 ~ 129.

Bau M, Dulski P. 1999. Comparing yttrium and rare earths in hydrothermal fluids from the Mid-Atlantic Ridge: Implications for Y and REE behaviour during near-vent mixing and for the Y/Ho ratio of Proterozoic seawater. Chemical Geology, 155: 77 ~ 90.

Becker R H, Clayton R N. 1976. Oxygen isotope study of a Precambrian banded iron-formation, Hamersley Range, Western Australia. Geochimica et Cosmochimica Acta, 40(10): 1153 ~ 1165.

Bekker A, Holland H D, Wang P L, Rumble D, Stein H J, Hannah J L, Coetzee L L, Beukes N J. 2004. Dating the rise of atmospheric oxygen. Nature, 427: 117 ~ 120.

Bekker A, Kaufman A J. 2007. Oxidative forcing of global climate change: A biogeochemical record across the oldest Paleoproterozoic ice age in North America. Earth and Planetary Science Letters, 258: 486 ~ 499.

Bekker A, Slack J F, Planavsky N, Krapežz B, Hofmann A, Konhauser K O, Rouxel O J. 2010. Iron formation: The sedimentary product of a complex interplay among mantle, tectonic, oceanic and biospheric processes. Economic Geology, 105: 467 ~ 508.

Bergquist B A, Boyle E A. 2006. Iron isotopes in the Amazon River system: Weathering and transport signatures. Earth and Planetary Science Letters, 248: 54 ~ 68.

Bern C R, Brzezinski M A, Beucher C P, Ziegler K, Chadwick O A. 2010. Weathering, dust, and biocycling effects on soil silicon isotope ratios. Geochimica et Cosmochimica Acta, 74: 876 ~ 889.

Bolhar R, Kranendonk M J V, Kamber B S. 2005. A trace element study of siderite—jasper banded iron formation in the 3.45Ga Warrawoona Group, Pilbara Craton: Formation from hydrothermal ? uids and shallow seawater. Precambrian Research, 137: 93 ~ 114.

Bontognali T R R, Fischer W W, Follmi K B. 2013. Siliciclastic associated banded iron formation from the 3.2 Ga Moodies Group, Barberton Greenstone Belt, South Africa. Precambrian Research, 226: 116 ~ 124.

Brocks J J, Logan G A, Buick R, Summons R E. 1999. Archean molecular fossils and the early rise of eukaryotes. Science, 185: 1033 ~ 1036.

Buick R. 1992. The antiquity of oxygenic photosynthesis: Evidence from stromatolites in sulphate-deficient Archaean lakes. Science, 255: 74 ~ 77.

Buick R. 2008. When did oxygenic photosynthesis evolve? Philosophical Transactions of the Royal Society of London, 363: 2731 ~ 2743.

Bullen T D, White A F, Childs C W, Vivit D V, Schulz M S. 2001. Demonstration of significant abiotic iron isotope fractionation in nature. Geology, 29: 699 ~ 702.

Cabral A R, Zeh A, Koglin N, Gomes J A A S, Viana D J, Lehmann B. 2012. Dating the Itabira iron formation, Quadrilátero Ferrífero of Minas Gerais, Brazil, at 2.65 Ga: Depositional U-Pb age of zircon from a metavolcanic layer. Precambrian Research, 204 ~ 205: 40 ~ 45.

Cairns-Smith A G. 1978. Precambrian solution photochemistry, inverse segregation, and banded iron formations. Nature, 76: 807 ~ 808.

Canfield D E, Teske A. 1996. Late Proterozoic rise in atmospheric oxygen concentration inferred from phylogenetic and sulphur-isotope studies. Nature, 382: 127 ~ 132.

Canfield D E. 1998. A new model for Proterozoic ocean chemistry. Nature, 396: 450 ~ 453.

Canfield D E. 2005. The early history of atmospheric oxygen. Annual Review of Earth and Planetary Sciences, 33: 1 ~ 36.

Cannon W F, Schulz K J, Horton J W, Kring D A. 2010. The Sudbury impact layer in the Paleoproterozoic iron ranges of northern Michigan, USA. Geological Society of America Bulletin, 122: 50 ~ 75.

Chen Guangyuan, Li Meihua, Wang Xuefang. 1984#. Special issue on genetic mineralogy of iron ore in Gongchangling. Minerals and Rocks, 4(2): 74 ~ 109.

Chen Jing, Li Houmin, Luo Dike, Li Lixing, Yang Xiuqing, Liu Mingjun, Yao Tong, Hu Bin. 2015&. Formation age, geochemical characteristics and geological significance of the Zhalanzhangzi BIF in eastern Hebei Province. Geological Bulletin of China, 34(5): 919 ~ 929.

Chen Liang. 2007&. Geochemistry and chronology of the Guyang Greenstone Belt. Tutor: Guo Jinghui, Zhai Mingguo. Beijing: Institute of Geology and Geophysics, Chinese Academy of Sciences, Postdoctorial Research Report, 1 ~ 40.

Chen Yuqi. 1957&. Problems on the genesis of the high-grade ore in the pre-Sinian (pre-Cambrian) banded iron ore deposits of the Anshan-type of Liaoning and Shantung provinces. Acta Geologica Sinica, 37(2): 153 ~ 189.

Cloud P E. 1968. Atmospheric and hydrospheric evolution on the primitive earth. Science, 160: 729 ~ 736.

Cloud P E. 1973. Paleoecological significance of banded iron-formation. Economic Geology, 68: 1135 ~ 1143.

Clout J M F. 2003. Upgrading processes in BIF-derived iron ore deposits: Implications for ore genesis and downstream processing. Applied Earth Science, 112: 89 ~ 95.

Clout J M F, Simonson B M. 2005. Precambrian iron formations and iron formation-hosted iron ore deposits. Economic Geology, 100: 643 ~ 679.

Condie K C. 1997. Plate Tectonics and Crustal Evolution. Butterworth—Heinemann, Oxford: 1 ~ 282.

Cui Minli, Zhang Lianchang, Wu Huaying, Xu Yingxia, Li Wenjun. 2014. Timing and tectonic setting of the Sijiaying banded iron deposit in the eastern Hebei province, North China Craton: Constraints from geochemistry and SIMS zircon U-Pb dating. Journal of Asian Earth Sciences, 94: 240 ~ 251.

Czaja A D, Johnson C M, Beard B L, Roden E E, Li W Q, Moorbath S. 2013. Biological Fe oxidation controlled deposition of banded iron formation in the ca. 3770 Ma Isua Supracrustal Belt (West Greenland). Earth and Planetary Science Letters, 363: 192 ~ 203.

Dai Yanpei, Zhang Liangchang, Wang Changle, Liu Li, Cui Minli, Zhu Mingtian, Xiang Peng. 2012&. Genetic type, formation age and tectonic setting of the Waitoushan banded iron formation, Benxi, Liaoning province. Acta Petrologica Sinica, 28(11): 3574 ~ 3594.

Dai Yanpei, Zhang Liangchang, Zhu Mingtian, Wang Changle, Liu Li.

2013&. Chentaigou BIF-type iron deposit, Anshan area associated with Archean crustal growth: constraints from zircon U-Pb dating and Hf isotope. Acta Petrologica Sinica, 29(7): 2537 ~ 2550.

Dai Yanpei, Zhang Lianchang, Zhu Mingtian, Wang Changle, Liu Li, Xiang Peng. 2014. The composition and genesis of Mesoarchean Dagushan banded iron formation in the Anshan area, the North China Craton. Ore Geology Review, 63: 353 ~ 373.

Dai Yanpei. 2014&. The Archean two-stage BIF deposition and genesis of high-grade iron ores in the Anshan—Benxi area. Tutor: Zhang Lianchang. Beijing: Institute of Geology and Geophysics, Chinese Academy of Sciences, Doctoral Dissertation, 1 ~ 166.

Dauphas N, Rouxel O. 2006. Mass spectrometry and natural variations of iron isotopes. Mass Spectrom. Rev., 25: 515 ~ 550.

Dauphas N, Cates N L, Mojzsis S J, Busigny V. 2007. Identification of chemical sedimentary protoliths using iron isotopes in the > 3750 Ma Nuvvuagittuq supracrustal belt, Canada. Earth and Planetary Science Letters, 254: 358 ~ 376.

Dobson D P, Brodholt J P. 2005. Subducted banded iron formations as a source of ultralow-velocity zones at the core—mantle boundary. Nature, 434: 371 ~ 374.

Dong Chunyan, Wan Yusheng, Xu Zhongyuan, Liu Dunyi, Yang Zhensheng, Ma Mingzhu, Xie Hangqiang. 2012#. SHRIMP zircon U-Pb dating of late Paleoproterozoic kondalites in the Daqing Mountain area on North China Craton. Scicence China: Earth Sciences, 42(12): 1851 ~ 1862.

Dong Xiaojie, Xu Zhongyuan, Liu Zhenghong, Sha Qian. 2012. Zircon U-Pb geochronology of Archean high-grade metamorphic rocks from Xi Ulanbulang area, central Inner Mongolia. Science China Earth Sciences, 55(2): 204 ~ 212.

Douville E, Bienvenu P, Charlou J L, Donval J P, Fouquet Y, Appriou P, Gamo T. 1999. Yttrium and rare earth elements in fluids from various deep-sea hydrothermal systems. Geochimica et Cosmochimica Acta, 63: 627 ~ 643.

Drever J I. 1974. Geochemical model for the origin of Precambrian banded iron formations. Geological Society of America Bulletin, 85: 1099 ~ 1106.

Duuring P, Hagemann S. 2013. Genesis of superimposed hypogene and supergene Fe orebodies in BIF at the Madoonga deposit, Yilgarn Craton, Western Australia. Mineralium Deposita, 48(3): 371 ~ 395.

Dymek R F, Klein C. 1988. Chemistry, petrology, and origin of banded iron formation lithologies from the 3800 Ma Isua Supracrustal Belt, West Greenland. Precambrian Research, 39: 247 ~ 302.

Ehrenreich A, Widdel F. 1994. Anaerobic oxidation of ferrous iron by purple bacteria, a new type of phototrophic metabolism. Applied and Environmental Microbiology, 60: 4517 ~ 4526.

Eigenbrode J L, Freeman K H. 2006. Late Archean rise of aerobic microbial ecosystems. Proceedings of the National Academy of Sciences, 103: 15759 ~ 15764.

Eigenbrode J L, Freeman K H, Summons R E. 2008. Methylhopane biomarker hydrocarbons in Hamersley Province sediments provide evidence for Neoarchean aerobiosis. Earth and Planetary Science Letters, 273: 323 ~ 331.

Emerson D, Moyer C L. 2002. Neutrophilic Fe-oxidizing bacteria are abundant at the Loihi seamount hydrothermal vents and play a major role in Fe oxide deposition. Applied and Environmental Microbiology, 68: 3085 ~ 3093.

Ewers W E, Morris R C. 1981. Studies of the Dales Gorge Member of the Brockman Iron Formation, Western Australia. Economic Geology, 76: 1929 ~ 1953.

Fairchild I J, Kennedy M J. 2007. Neoproterozoic glaciation in the Earth system. Journal of the Geological Society of London, 164: 895 ~ 921.

Farquhar J, Bao H M, Thiemens M. 2000. Atmospheric influence of Earth's earliest sulphur cycle. Science, 289: 756 ~ 758.

Foustoukos D I, Bekker A. 2008. Hydrothermal Fe(II) oxidation during phase separation: relevance to the origin of Algoma-type BIFs. Goldschmidt 2008 Conference, Vancouver BC, Canada. Geochimica et Cosmochimica Acta, 72(S1): A280.

Frei R, Polat A. 2007. Source heterogeneity for the major components of ~ 3.7 Ga banded iron formations (Isua Greenstone Belt, Western Greenland): Tracing the nature of interacting water masses in BIF formation. Earth and Planetary Science Letters, 253: 266 ~ 281.

Frei R, Dahl P S, Duke E F, Frei K M, Hansen T R, Frandsson M M, Jensen L A. 2008. Trace element and isotopic characterization of Neoarchaean and Paleoproterozoic iron formations in the Black Hills (South Dakota, USA): Assessment of chemical change during 2.9 ~ 1.9 Ga deposition bracketing the 2.4 ~ 2.2 Ga first rise of atmospheric oxygen. Precambrian Research, 162: 441 ~ 474.

Frimmel H E. 2005. Archaean atmospheric evolution: evidence from the Witwatersrand gold fields, South Africa. Earth Science Reviews, 70: 1 ~ 46.

Garrels R M. 1987. A model for the deposition of the microbanded Precambrian iron formations. American Journal of Science, 287: 81 ~ 106.

Georg R B, Halliday A N, Schauble E A, Reynolds B C. 2007. Silicon in the Earth's core. Nature, 447: 1102 ~ 1106.

German C R, Masuzawa T, Greaves M J, Elderfield H, Edmond J M. 1995. Dissolved rare earth elements in the Southern Ocean: Cerium oxidation and the influence of hydrography. Geochimica et Cosmochimica Acta, 59: 1551 ~ 1558.

Glikson A, Vickers J. 2007. Asteroid mega-impacts and Precambrian banded iron formations: 2.63 Ga and 2.56 Ga impact ejecta/fallout at the base of BIF/argillite units, Hamersley Basin, Pilbara Craton, Western Australia. Earth and Planetary Science Letters, 254: 214 ~ 226.

Glikson A. 2010. Archaean asteroid impacts, banded iron formations and MIF—S anomalies: A discussion. Icarus, 207: 39 ~ 44.

Gross G A. 1980. A classification of iron formations based on depositional environments. The Canadian Mineralogist, 18: 215 ~ 222.

Gross G A. 1983. Tectonic systems and the deposition of iron-formation. Precambrian Research, 20: 171 ~ 187.

Gross G A. 1996. Algoma-type previous term iron-formation. Next term, in: Lefebure D, Höy T. Eds. Selected British Columbia Mineral Deposits Profiles 2. British Columbia Ministry of Employment and Investment Open File, Ottawa: 25 ~ 28.

Guan Guangyue. 1961#. The significance of metamorphism on formation of the high-grade iron ores in the Anshan-type iron deposits. Acta Geologica Sinica, 41(1): 65 ~ 76.

Habicht K S, Gade M, Thamdrup B, Berg P, Canfield D E. 2002. Calibration of sulfate levels in the Archean ocean. Science, 298: 2372 ~ 2374.

Halverson G P, Poitrasson F, Hoffman P F, Nédélec A, Montel J M, Kirby J. 2011. Fe isotope and trace element geochemistry of the Neoproterozoic syn-glacial Rapitan iron formation. Earth and

Planetary Science Letters, 309: 100 ~ 112.

Hamade T, Konhauser K O, Raiswell R, Goldsmith S, Morris R C. 2003. Using Ge/Si ratios to decouple iron and silica fluxes in Precambrian banded iron formations. Geology, 31: 35 ~ 38.

Han T M, Runnegar B. 1992. Megascopic eukaryotic alage from the 2.1 billion-year-old Negaunee iron-formation, Michigan. Science, 257: 232 ~ 235.

Han Chunming, Xiao Wenjiao, Su Benxun, Chen Zhengle, Zhang Xiaohui, Ao Songjian, Zhang Jien, Zhang Zhiyong, Wan Bo, Song Dongfang, Wang Zhongmei. 2014a. Neoarchean Algoma-type banded iron formations from Eastern Hebei, North China Craton: SHRIMP U-Pb age, origin and tectonic setting. Precambrian Research, 251: 212 ~ 231.

Han Chunming, Xiao Wenjiao, Su Benxun, Sakyi P A, Chen Zhengle, Zhang Xiaohui, Ao Songjian, Zhang Jien, Wan Bo, Zhang Zhiyong, Wang Zhongmei, Ding Jiaxin. 2014b. Formation age and genesis of the Gongchangling Neoarchean banded iron deposit in eastern Liaoning Province: Constraints from geochemistry and SHRIMP zircon U-Pb dating. Precambrian Research, 254: 306 ~ 322.

Harder E C. 1919. Iron-depositing bacteria and their geological relations. U. S. Geological Survey Professional Paper, 113: 1 ~ 89.

Haugaard R, Frei R, Stendal H, Konhauser K. 2013. Petrology and geochemistry of the ~ 2.9 Ga Itilliarsuk banded iron formation and associated supracrustal rocks, West Greenland: Source characteristics and depositional environment. Precambrian Research, 229: 150 ~ 176.

Heck P R, Huberty J M, Kita N T, Ushikubo T, Kozdon R, Valley J W. 2011. SIMS analyses of silicon and oxygen isotope ratios for quartz from Archean and Paleoproterozoic banded iron formations. Geochimica et Cosmochimica Acta, 75: 5879 ~ 5891.

Heising S, Richter L, Ludwig W, Schink B. 1999. Chlorobium ferrooxidans sp. nov., a phototrophic green sulfur bacterium that oxidizes ferrous iron in coculture with a "Geospirillum" sp. strain. Archives of Microbiology, 172(2): 116 ~ 124.

Hoffman P F, Kaufman A J, Halverson G P, Schrag D P. 1998. A Neoproterozoic snowball Earth. Science, 281: 1342 ~ 1346.

Holland H D. 1973. The oceans: A possible source of iron in iron-formations. Economic Geology, 68: 1169 ~ 1172.

Holland H D. 1984. The chemical evolution of the atmosphere and oceans. New York, Princeton University Press: 1 ~ 582.

Holland H D. 2002. Volcanic gases, black smokers, and the Great Oxidation Event. Geochimica et Cosmochimica Acta, 66: 3811 ~ 3826.

Holland H D. 2006. The oxygenation of the atmosphere and oceans. Philosophical Transactions of the Royal Society B: Biological Sciences, 361 (1470): 903 ~ 915.

Hou Kejun, Li Yanhe, Wan Defang. 2007#. Constraints on the Archean atmospheric oxygen and sulfur cycle from mass-independent sulfur records from Anshan—Benxi BIFs, Liaoning Province, China. Scicence China: Earth Sciences, 37(8): 997 ~ 1003.

Hou Kejun, Li Yanhe, Gao Jianfeng, Liu Feng, Qin Yan. 2014. Geochemistry and Si—O—Fe isotope constraints on the origin of banded iron formations of the Yuanjiacun Formation, Lvliang Group, Shanxi, China. Ore Geology Reviews, 57: 288 ~ 298.

Housen B A, Van Der Pluijm B A, Essene E J. 1995. Plastic behavior of magnetite and high strains obtained from magnetic fabrics in the Parry Sound shear zone, Ontario Grenville Province. Journal of Structural Geology, 17: 265 ~ 278.

Huston D L, Logan G A. 2004. Barite, BIFs and bugs: Evidence for the evolution of the Earth′s early hydrosphere. Earth and Planetary Science Letters, 220: 41 ~ 55.

Isley A E. 1995. Hydrothermal plumes and the delivery of iron to banded iron formation. The Journal of Geology, 103: 169 ~ 185.

Isley A E, Abbott D H. 1999. Plume-related mafic volcanism and the deposition of banded iron formation. Journal of Geophysical Research: Solid Earth (1978 ~ 2012), 104: 15461 ~ 15477.

Jacobsen S B, Pimentel-Klose M R. 1988a. A Nd isotopic study of the Hamersley and Michipicoten banded iron formations: the source of REE and Fe in Archean oceans. Earth and Planetary Science Letters, 87: 29 ~ 44.

Jacobsen S B, Pimentel-Klose M R. 1988b. Nd isotopic variations in Precambrian banded iron formations. Geophysical Research Letters, 15: 393 ~ 396. James H L. 1954. Sedimentary facies of iron-formation. Economic Geology, 49: 235 ~ 293.

James H L. 1969. Comparison between Red Sea deposits and older ironstone and iron formation, in Degens ET, Ross DA, eds., Hot brines and recent heavy metal deposits in the Red Sea. New York: Springer-Verlag: 525 ~ 532.

James H L. 1983. Distribution of banded iron-formation in space and time. In: Trendall AF, Morris RC (Eds), Developments in Precambrian Geology, 6: 471 ~ 490.

Jenner F E, Bennett V C, Nutman A P, Friend C R L, Norman M D, Yaxley G. 2009. Evidence for subduction at 3.8 Ga: Geochemistry of arc-like metabasalts from the southern edge of the Isua Supracrustal Belt. Chemical Geology, 261: 83 ~ 98.

Jiang Shaoyong, Ding Tiping, Wan Defang, Li Yanhe. 1992#. Silicon isotopic compositions of Archean banded Si—Fe formation (BIF) in the Gongchangling Ore deposit, Liaoning Province, China. Scicence China (Series B), (6): 626 ~ 631.

Johnson C M, Skulan J L, Beard B L, Sun H, Nealson K H, Braterman P S. 2002. Isotopic fractionation between Fe(III) and Fe(II) in aqueous solutions. Earth and Planetary Science Letters, 195: 141 ~ 153.

Johnson C M, Beard B L, Klein C, Beukes N J, Roden E E. 2008. Iron isotopes constrain biologic and abiologic processes in banded iron formation genesis. Geochimica et Cosmochimica Acta, 72: 151 ~ 169.

Kappler A, Newman D K. 2004. Formation of Fe(III)-minerals by Fe(II)-oxidizing photoautotrophic bacteria. Geochimica et Cosmochimica Acta, 68: 1217 ~ 1226.

Kappler A, Pasquero C, Konhauser K O, Newman D K. 2005. Deposition of banded iron formations by anoxygenic phototrophic Fe(II)-oxidizing bacteria. Geology, 33: 865 ~ 868.

Kasting J F. 1993. Earth′s early atmosphere. Science, 259: 920 ~ 926.

Kasting J F. 2001. Earth history: The rise of atmospheric oxygen. Science, 293: 819 ~ 820.

Kasting J F. 2013. What caused the rise of atmospheric O_2? Chemical Geology, 362: 13 ~ 25.

Kato Y, Ohta I, Tsunematsu T, Watanabe Y, Isozaki Y, Maruyama S, Imai N. 1998. Rare earth element variations in mid-Archean banded iron formations: implications for the chemistry of ocean and plate tectonics. Geochimica et Cosmochimica Acta, 62: 3475 ~ 3497.

Katsuta N, Shimizu I, Helmstaedt H, Takano M, Kawakami S, Kumazawa M. 2012. Major element distribution in Archean banded iron formation (BIF): Influence of metamorphic differentiation.

Journal of Metamorphic Geology, 30: 457 ~ 472.

Khan R M K, Das Sharma S, Patil D J, Naqvi S M. 1996. Trace, rare-earth element, and oxygen isotopic systematics for the genesis of banded iron-formations: Evidence from Kushtagi schist belt, Archaean Dharwar Craton, India. Geochimica et Cosmochimica Acta, 60: 3285 ~ 3294.

Klein C, Beukes N J. 1989. Geochemistry and sedimentology of a facies transition from limestone to iron-formation deposition in the Early Proterozoic Transvaal Supergroup, South Africa. Economic Geology, 84: 1733 ~ 1774.

Klein C, Beukes N J. 1993. Sedimentology and geochemistry of the glaciogenic late Proterozoic Rapitan iron-formation in Canada. Economic Geology, 88: 542 ~ 565.

Klein C. 2005. Some Precambrian banded iron-formations (BIFs) from around the world: Their age, geologic setting, mineralogy, metamorphism, geochemistry, and origin. American Mineralogist, 90: 1473 ~ 1499.

Klinkhammer G P, Elderfield H, Edmond J M, Mitra A. 1994. Geochemical implications of rare earth element patterns in hydrothermal fluids from mid-ocean ridges. Geochimica et Cosmochimica Acta, 58: 5105 ~ 5113.

Konhauser K O, Hamade T, Raiswell R, Morris R C, Ferris F G, Southam G, Can? eld D E. 2002. Could bacteria have formed the Precambrian banded iron-formations? Geology, 30: 1079 ~ 1082.

Konhauser K O, Amskold L, Lalonde S V, Posth N R, Kappler A, Anbar A. 2007. Decoupling photochemical Fe(II) oxidation from shallow-water BIF deposition. Earth and Planetary Science Letters, 258: 87 ~ 100.

Konhauser K O, Pecoits E, Lalonde S V, Papineau D, Nisbet E G, Barley M E, Arndt N T, Zahnle K, Kamber B S. 2009. Oceanic nickel depletion and a methanogen famine before the Great Oxidation Event. Nature, 458: 750 ~ 753.

Krapež B, Barley M E, Pickard A L. 2003. Hydrothermal and resedimented origins of the precursor sediments to banded iron formation: Sedimentological evidence from the Early Palaeoproterozoic Brockman Supersequence of Western Australia. Sedimentology, 50: 979 ~ 1011.

Kump L R, Seyfried W E. 2005. Hydrothermal Fe fluxes during the Precambrian: Effect of lowoceanic sulfate concentrations and lowhydrostatic pressure on the composition of black smokers. Earth and Planetary Science Letters, 235: 654 ~ 662.

Lai Xiaodong, Yang Xiaoyong. 2012&. Characteristics of the banded iron formation (BIF) and its zircon chronology in Yangzhuang, western Shandong. Acta Petrologica Sinica, 28(11): 3612 ~ 3622.

Lan Tingguang, Fan Hongrui, Hu Fangfang, Yang Kuifeng, Zheng Xiaoli, Zhang Huadong. 2012&. Geological and geochemical characteristics of Paleoproterozoic Changyi banded iron formation deposit, Jiaodong Peninsula of eastern China. Acta Petrologica Sinica, 28(11): 3595 ~ 3611.

Lan Tingguang, Fan Hongrui, Santosh M, Hu Fangfang, Yang Kuifeng, Liu Yongsheng. 2014a. U-Pb zircon chronology, geochemistry and isotopes of the Changyi banded iron formation in the eastern Shandong Province: Constraints on BIF genesis and implications for Paleoproterozoic tectonic evolution of the North China Craton. Ore Geology Reviews, 56: 472 ~ 486.

Lan Tingguang, Fan Hongrui, Hu Fangfang, Yang Kuifeng, Cai Yachun, Liu Yongsheng. 2014b. Depositional environment and tectonic implications of the Paleoproterozoic BIF in Changyi area, eastern North China Craton: Evidence from geochronology and geochemistry of the metamorphic wallrocks. Ore Geology Reviews, 61: 52 ~ 72.

Leith C K. 1903. The Mesabi iron-bearing district of Minnesota. U. S. Geological Survey Monograph, 43: 1 ~ 316.

Li Houmin, Liu Mingjun, Li Lixing, Yang Xiuqing, Chen Jing, Yao Liangde, Hong Xuekuan, Yao Tong. 2012&. Geology and geochemistry of the marble in the Gongchangling iron deposit in Liaoning Province and their metallogenic significance. Acta Petrologica Sinica, 28(11): 3497 ~ 3512.

Li Houmin, Zhang Zengjie, Li Lixing, Zhang Zhaochong, Chen Jing, Yao Tong. 2014. Types and general characteristics of the BIF-related iron deposits in China. Ore Geology Reviews, 57: 264 ~ 287.

Li Houmin, Yang Xiuqing, Li Lixing, Zhang Zhaochong, Liu Mingjun, Yao Tong, Chen Jing. 2015. Desilicification and iron activation—reprecipitation in the high-grade magnetite ores in BIFs of the Anshan—Benxi area, China: Evidence from geology, geochemistry and stable isotopic characteristics. Journal of Asian Earth Sciences, 113: 998 ~ 1016.

Li Lixing, Li Houmin, Xu Yingxia, Chen Jing, Yao Tong, Zhang Longfei, Yang Xiuqing, Liu Mingjun. 2015. Zircon growth and ages of migmatites in the Algoma-type BIF-hosted iron deposits in Qianxi Group from eastern Hebei Province, China: Timing of BIF deposition and anatexis. Journal of Asian Earth Sciences, 113: 1017 ~ 1034.

Li Shaobing. 1979&. A contribution to the genesis of rich magnetite deposit of the Gongchangling type: in the light of graphite discovered in it. Geochimica, (2): 170 ~ 177.

Li Shuguang, Zhi Xiachen, Chen Jiangfeng, Wang Junxin, Deng Yanyao. 1983&. Origin of graphites in early Precambrian banded iron formation in Anshan, China. Geochimica, (2): 162 ~ 169.

Li Yanhe, Hou Kejun, Wan Defang, Zhang Zengjie, Le Guoliang. 2010&. Formation mechanism of Precambrian banded iron formation and atmosphere and ocean during early stage of the Earth. Acta Geologica Sinica, 84(9): 1359 ~ 1373.

Li Yanhe, Zhang Zengjie, Wu Jiashan, Shang Longping. 2011&. Metamorphic chronology of the BIF in Malanzhuang of eastern Hebei Province and its geological implications. Mineral Deposits, 30(4): 645 ~ 653.

Li Yanhe, Hou Kejun, Wan Defang, Zhang Zengjie. 2012&. A compare geochemistry study for Algoma- and Superior-type banded iron formations. Acta Petrologica Sinica, 28(11): 3513 ~ 3519.

Li Yanhe, Hou Kejun, Wan Defang, Zhang Zengjie, Yue Guoliang. 2014. Precambrian banded iron formations in the North China Craton: Silicon and oxygen isotopes and genetic implications. Ore Geology Reviews, 57: 299 ~ 307.

Li Yiliang. 2014. Micro- and nanobands in late Archean and Palaeoproterozoic banded-iron formations as possible mineral records of annual and diurnal depositions. Earth and Planetary Science Letters, 391: 160 ~ 170.

Li Zhihong, Zhu Xiangkun, Tang Suohan. 2008&. Characters of Fe isotopes and rare earth elements of banded iron formations from Anshan—Benxi area: implications for Fe source. Acta Petrologica et Mineralogica, 27(4): 285 ~ 290.

Li Zhihong, Zhu Xiangkun, Tang Suohan. 2012&. Fe isotope compositions of banded iron formation from Anshan—Benxi area: constraints on the formation mechanism and Archean ocean

environment. Acta Petrologica Sinica, 28(11): 3545 ~ 3558.

Liu Jun, Jin Shuyun. 2010&. Genesis study of magnetite-rich ore in Gongchangling iron deposit, Liaoning. Geoscience, 24(1): 80 ~ 88.

Liu Li, Zhang Lianchang, Dai Yanpei, Wang Changle, Li Zhiquan. 2012&. Formation age, geochemical signatures and geological significance of the Sanheming BIF-type iron deposit in the Guyang greenstone belt, Inner Mongolia. Acta Petrologica Sinica, 28(11): 3623 ~ 3637.

Liu Li, Zhang Lianchang, Dai Yanpei. 2014. Formation age and genesis of the banded iron formations from the Guyang Greenstone Belt, Western North China Craton. Ore Geology Reviews, 63: 388 ~ 404.

Liu Lei, Yang Xiaoyong. 2015. Temporal, environmental and tectonic signi? cance of the Huoqiu BIF, southeastern North China Craton: Geochemical and geochronological constraints. Precambrian Research, 261: 217 ~ 233.

Liu Mingjun. 2013&. Hydrothermal metasomatism and its metallogenic significance of the Gongchangling iron deposit, Liaoning, China. Tutor: Xue Chunji, Li Houmin. Beijing: China University of Geosciences (Beijing), Master degree thesis, 1 ~ 113.

Liu Shuwen, Santosh M, Wang Wei, Bai Xiang, Yang Pengtao. 2011. Zircon U-Pb chronology of the Jianping Complex: Implications for the Precambrian crustal evolution history of the northern margin of North China Craton. Gondwana Research, 20: 48 ~ 63.

Liu Shuwen, Zhang Jian, Li Qiugen, Zhang Lifei, Wang Wei, Yang Pengtao. 2012. Geochemistry and U-Pb zircon ages of metamorphic volcanic rocks of the Paleoproterozoic Lüliang Complexand constraints on the evolution of the Trans-North China Orogen, North China Craton. Precambrian Research, 222: 173 ~ 190.

Liu Y G, Miah M R U, Schmitt R A. 1988. Cerium: A chemical tracer for paleo-oceanic redox conditions. Geochimica et Cosmochimica Acta, 52: 1361 ~ 1371.

Lu Songnian, Yang Chunliang, Li Huaikun, Jiang Mingmei, Chen Anshu, Hu Zhengde. 1995&. Sm-Nd isotopic information of Precambrian metabasement in the North China Platform. Journal of Geology and Mineral Resources of North China, 10(2): 143 ~ 153.

Ma Xudong, Fan Hongrui, Santosh M, Guo Jinghui. 2014. Chronology and geochemistry of Neoarchean BIF-type iron deposits in the Yinshan Block, North China Craton: Implications for oceanic ridge subduction. Ore Geology Reviews, 63: 405 ~ 417.

Mamtani M A, Piazolo S, Greiling R O, Kontny A, Hrouda F. 2011. Process of magnetite fabric development during granite deformation. Earth and Planetary Science Letters, 308: 77 ~ 89.

McLennan S M. 1989. Rare earth elements in sedimentary rocks: influence of provenance and sedimentary processes. In: Lipin BR and McKay GA (Eds.), Geochemistry and mineralogy of rare earth elements. Reviews in Mineralogy and Geochemistry, 21: 169 ~ 200.

Mloszewska A M, Pecoits E, Cates N L, Mojzsis S J, O'Neil J, Robbins L J, Konhauser K O. 2012. The composition of Earth's oldest iron formations: The Nuvvuagittuq Supracrustal Belt (Québec, Canada). Earth and Planetary Science Letters, 317 ~ 318: 331 ~ 342.

Morris R C. 1983. Supergene alteration of banded iron formation. Developments in Precambrian geology, 6: 513 ~ 534.

Morris R C. 1985. Genesis of iron ore in banded iron-formation by supergene and supergene—metamorphic process: A conceptual model. In: Wolf KH (Ed.), Handbook Stratabound and Stratiform Ore Deposits, 13: 73 ~ 235.

Morris R C. 1998. BIF-hosted iron ore deposits ~ Hamersley style. AGSO Journal of Australian Geology and Geophysics, 17: 207 ~ 212.

Müller S G, Krapež B, Barley M E, Fletcher I R. 2005. Giant iron-ore deposits of the Hamersley province related to the breakup of Paleoproterozoic Australia: New insights from in situ SHRIMP dating of baddeleyite from mafic intrusions. Geology, 33: 577 ~ 580.

Nold J L, Davidson P, Dudley M A. 2013. The pilot knob magnetite deposit in the Proterozoic St. Francois Mountains Terrane, southeast Missouri, USA: A magmatic and hydrothermal replacement iron deposit. Ore Geology Reviews, 53: 446 ~ 469.

Nutman A P, Wang Y S, Du L L, Friend C R L, Dong C Y, Xie H Q, Wang W, Sun H Y, Liu D Y. 2011. Multistage late Neoarchaean crustal evolution of the North China Craton, eastern Hebei. Precambrian Research, 189: 43 ~ 65.

Ohmoto H, Watanabe Y, Kumazawa K. 2004. Evidence from massive siderite beds for a CO_2-rich atmosphere before ~ 1.8 billion years ago. Nature, 429: 395 ~ 399.

Ohmoto H, Watanabe Y, Yamaguchi K E, Naraoka H, Haruna M, Kakegawa T, Hayashi K, Kato Y. 2006. Chemical and biological evolution of early Earth: Constraints from banded iron formations. Geological Society of America Memoir, 198: 291 ~ 331.

Ohtomo Y, Kakegawa T, Ishida A, Nagase T, Rosing M T. 2014. Evidence for biogenic graphite in early Archaean Isua metasedimentary rocks. Nature Geoscience, 7: 25 ~ 28.

Ono S, Fayek M, Ohmoto H. 2000. Origin of uraninite in the Elliot lake district, Canada and the atmospheric oxygen level of 2.3 Ga Earth. Evolution of the Atmosphere, Ocean, Crust and Biosphere: 67 ~ 74.

Pecoits E, Gingras M K, Barley M E, Kappler A, Posth N R, Konhauser K O. 2009. Petrography and geochemistry of the Dales Gorge banded iron formation: Paragenetic sequence, source and implications for palaeo-ocean chemistry. Precambrian Research, 172: 163 ~ 187.

Pickard A L. 2002. SHRIMP U-Pb zircon ages of tuffaceous mudrocks in the Brockman Iron Formation of the Hamersley Range, Western Australia. Aust. J. Earth Sci., 49: 491 ~ 507.

Planavsky N, Rouxel O J, Bekker A, Shapiro R, Fralick P, Knudsen A. 2009. Iron-oxidizing microbial ecosystems thrived in late Paleoproterozoic redox-stratified oceans. Earth Planet. Sci. Lett., 286: 230 ~ 242.

Planavsky N, Rouxel O J, Bekker A, Hofmann A, Little C T S, Lyons T W. 2012. Iron isotope composition of some Archean and Proterozoic iron formations. Geochimica et Cosmochimica Acta, 80: 158 ~ 169.

Posth N R, Hegler F, Konhauser K O, Kappler A. 2008. Alternating Si and Fe deposition caused by temperature fluctuations in Precambrian oceans. Nature Geoscience, 1: 703 ~ 708.

Posth N R, Canfield D E, Kappler A. 2014. Biogenic Fe (III) minerals: from formation to diagenesis and preservation in the rock record. Earth-Science Reviews, 135: 103 ~ 121.

Poulton S W, Fralick P W, Can? eld D E. 2004. The transition to a sulphidic ocean similar to 1.84 billion years ago. Nature, 431: 173 ~ 177.

Qiao Guangsheng, Zhai Mingguo, Yan Yuehua. 1990&. Geochronological study of Archaean rocks in Anshan, Liaoning province. Scientia Geologica Sinica, 2(2): 158 ~ 164.

Qu Junfeng, Li Jinyi, Liu Jianfeng. 2013&. Formation age of the BIF

from the Wangsiyu iron deposit, eastern Hebei Province, and its implication. Geologcal Bulletin OF China, 32(2~3): 260~266.

Rao T G, Naqvi S M. 1995. Geochemistry, depositional environment and tectonic setting of the BIFs of the Late Archaean Chitradurga Schist Belt, India. Chemical Geology, 121: 217~243.

Rasmussen B, Fletcher I R, Bekker A, Muhling J R, Gregory C J, Thorne A M. 2012. Deposition of 1. 88-billion-year-old iron formations as a consequence of rapid crustal growth. Nature, 484: 498~501.

Rasmussen B, Meier D B, Krapež B, Muhling J R. 2013. Iron silicate microgranules as precursor sediments to 2.5-billion-year-old banded iron formations. Geology, 41: 435~438.

Ribeiro da Luz B, Crowley J K. 2012. Morphological and chemical evidence of stromatolitic deposits in the 2.75 Ga Carajas banded iron formation, Brazil. Earth and Planetary Science Letters, 355~356: 60~72.

Ripley E M, Shafer P, Li C, Hauck S A. 2008. Re-Os and O isotopic variations in magnetite from the contact zone of the Duluth Complex and the Biwabik Iron Formation, northeastern Minnesota. Chemical Geology, 249: 213~226.

Rona P A, Scott S D. 1993. A special issue on sea-floor hydrothermal mineralization: New perspective. Economic Geology, 88: 1935~1976.

Rye R, Holland H D. 1998. Paleosols and the evolution of atmospheric oxygen: A critical review. Am. J. Sci., 298: 621~672.

Seibold E. 1958. Jahreslagen in Sedimenten der mittleren Adria. Geologische Rundschau, 47: 100~117.

Severmann S, Johnson C M, Beard B L, German C R, Edmonds H N, Chiba H, Green D R H. 2004. The effect of plume processes on the Fe isotope composition of hydrothermally derived Fe in the deep ocean as inferred from the Rainbow vent site, Mid-Atlantic Ridge, 36 degrees 14′N. Earth and Planetary Science Letters, 225: 63~76.

Shen Baofeng, Zhai Anmin, Chen Wenming, Yang Chunliang, Hu Xiaodie, Cao Xiulan, Gong Xiaohua. 2006&. The Precambrian mineralization of China. Beijing: Geological Publishing House, 1~362.

Shen Qihan. 1998 #. Geological characteristics and settings of the Precambrain banded magnetite quartzite in north China platform. Cheng Yuqi. Collected papers on Precambrain geology study of North China platform. Beijing: Geological Publishing House, 1~30.

Shen Qihan, Song Biao, Xu Huifen, Geng Yuansheng, Shen Kun. 2004&. Emplacement and metamorphism ages of the Caiyu and Dashan igneous bodies, Yishui county, Shandong province: zircon SHRIMP chronology. Geological Review, 50(3): 275~284.

Shen Qihan, Song Huixia, Zhao Ziran. 2009&. Characteristics of rare earth elements and trace elements in Hanwang Neoarchaean banded iron formations, Shandong province. Acta Geoscientica Sinica, 30(6): 693~699.

Shen Qihan, Song Huixia, Yang Chonghui, Wan Yusheng. 2011&. Petrochemical characteristics and geological significations of banded iron formations in the Wutai Mountain of Shanxi and Qian´an of eastern Hebei. Acta Petrologica et Mineralogica, 30(2): 161~171.

Shi Yuruo, Wilde S A, Zhao Xitao, Ma Yinsheng, Du Lilin, Liu Dunyi. 2012. Late Neoarchean magmatic and subsequent metamorphic events in the northern North China Craton: SHRIMP zircon dating and Hf isotopes of Archean rocks from Yunmengshan Geopark, Miyun, Beijing. Gondwana Research, 21: 785~800.

Shields G A, Webb G E. 2004. Has the REE composition of seawater changed over geological time? Chemical Geology, 204: 103~107.

Slack J F, Grenne T, Bekker A, Rouxel O J, Lindberg P A. 2007. Suboxic deep seawater in the late Paleoproterozoic: Evidence from hematitic chert and Fe formation related to sea floor-hydrothermal sulfide deposits, central Arizona, USA. Earth Planet. Sci. Lett., 255: 243~256.

Slack J F, Cannon W F. 2009. Extraterrestrial demise of banded iron formations 1.85 billion years ago. Geology, 37: 1011~1014.

Søgaard E G, Medenwaldt R, Abraham-Peskir J V. 2000. Conditions and rates of biotic and abiotic iron precipitation in selected Danish freshwater plants and microscopic analysis of precipitate morphology. Water Reasearch, 34: 2675~2682.

Song Biao, Nutman AP, Liu Dunyi, Wu Jiashan. 1996. 3800 to 2500 Ma crustal evolution in the Anshan area of Liaoning province, northeastern China. Precambrian Research, 78: 79~94.

Steinhoefel G, Horn I, Blanckenburg von F. 2009. Microscale tracing of Fe and Si isotope signatures in banded iron formation using femtosecond laser ablation. Geochim. Cosmochim. Acta, 73: 5343~5360.

Straub K L, Rainey F A, Widdel F. 1999. Rhodovulum iodosum sp. nov. and Rhodovulum robiginosum sp. nov., two new marine phototrophic ferrous-iron-oxidizing purple bacteria. International Journal of Systematic Bacteriology, 49: 729~735.

Sun Huiyi, Dong Chunyan, Xie Hangqiang, Wang Wei, Ma Mingzhu, Liu Dunyi, Nutman A, Wan Yusheng. 2010&. The formation age of the Neoarchean Zhuzhangzi and Dantazi groups in the Qinglong area, eastern Hebei province: evidence from SHRIMP U-Pb zircon dating. Geological Review, 56(6): 888~898.

Sun Jian, Zhu Xiangkun. 2015&. Fe isotope geochemistry of Earth surface system. Geological Review, 61(6): 1370~1382.

Sun Xiaohui, Zhu Xiaoqing, Tang Haoshu, Zhang Qian, Luo Taiyi. 2014a. The Gongchangling BIFs from the Anshan—Benxi area, NE China: Petrological—geochemical characteristics and genesis of high-grade iron ores. Ore Geology Reviews, 60: 112~125.

Sun Xiaohui, Zhu Xiaoqing, Tang Haoshu, Zhang Qian, Luo Taiyi, Han Tao. 2014b. Protolith reconstruction and geochemical study on the wall rocks of Anshan BIFs, Northeast China: Implications for the provenance and tectonic setting. Journal of Geochemical Exploration, 136: 65~75.

Sun Zhilei, Zhou Huaiyang, Glasby G P, Sun Zhixue, Yang Qunhui, Yin Xijie, Li Jiwei. 2013. Mineralogical characterization and formation of Fe—Si oxyhydroxide deposits from modern seafloor hydrothermal vents. American Mineralogist, 98: 85~97.

Trendall A F, Basei M A S, Delaeter J R, Nelson D R. 1998. SHRIMP zircon U-Pb constraints on the age of the Carajas formation, Para Group, Amazon Craton. Journal of South American Earth Sciences, 11: 265~277.

Trendall A F. 2009. The significance of iron-formation in the Precambrian stratigraphic record. Precambrian sedimentary environments: A modern approach to ancient depositional systems, 33~66.

Wan Yusheng. 1993&. The formation and evolvement of ferreous rock series of Gongchangling, Liaoning province. Beijing: Beijing Science and Technology Press, 1~99.

Wan Yusheng, Song Biao, Yang Chun, Liu Dunyi. 2005&. Zircon

SHRIMP U-Pb geochronology of Archaean rocks from the Fushun—Qingyuan area, Liaoning province and its geological significance. Acta Geologica Sinica, 79(1): 78 ~ 87.

Wan Yusheng, Wilde S A, Liu Dunyi, Yang Changxiu, Song Biao, Yin Xiaoyan. 2006. Further evidence for ~ 1.85 Ga metamorphism in the Central Zone of the North China Craton: SHRIMP U-Pb dating of zircon from metamorphic rocks in the Lushan area, Henan Province. Gondwana Research, 9: 189 ~ 197.

Wan Yusheng, Liu Dunyi, Wang Sshiyan, Zhao Xun, Dong Chunyan, Zhou Hongying, Yin Xiaoyan, Yang Changxiu, Gao Linzhi. 2009&. Early Precambrian crustal evolution in the Dengfeng area, Henan province (eastern China): constraints from geochemistry and SHRIMP U-Pb zircon dating. Acta Geologica Sinica, 83(7): 982 ~ 999.

Wan Yusheng, Dong Chunyan, Xie Hangqiang, Wang Shijin, Song Mingchun, Xu Zhongyuan, Wang Shiyan, Zhou Hongying, Ma Mingzhu, Liu Dunyi. 2012&. Formation ages of early Precambrian BIFs in the North China Craton: SHRIMP zircon U-Pb dating. Acta Geologica Sinica, 86(9): 1447 ~ 1478.

Wan Yusheng, Dong Chunyan, Liu Dunyi, Kroner A, Yang Chonghui, Wang Wei, Du Lilin, Xie Hangqiang, Ma Mingzu. 2012a. Zircon ages and geochemistry of late Neoarchean syenogranites in the North China Craton: A review. Precambrian Research, 222 ~ 223: 265 ~ 289.

Wan Yusheng, Wang Shijin, Liu Dunyi, Wang Wei, Kroner A, Dong Chunyan, Yang Enxiu, Zhou Hongying, Xie Hangqiang, Ma Mingzu. 2012b. Redefinition of depositional ages of Neoarchean supracrustal rocks in western Shandong Province, China: SHRIMP U-Pb zircon dating. Gondwana Research, 21: 768 ~ 784.

Wang Changle, Zhang Lianchang, Lan Caiyun, Dai Yanpei. 2014#. Rare earth element and yttrium compositions of the Paleoproterozoic Yuanjiacun BIF in the Lüliang area and their implications for the Great Oxidation Event (GOE). Science China: Earth Sciences, 44(11): 2389 ~ 2405.

Wang Changle, Zhang Lianchang, Lan Caiyun, Dai Yanpei. 2014. Petrology and geochemistry of the Wangjiazhuang banded iron formation and associated supracrustal rocks from the Wutai greenstone belt in the North China Craton: Implications for their origin and tectonic setting. Precambrian Research, 255: 603 ~ 626.

Wang Changle, Zhang Lianchang, Dai Yanpei, Lan Caiyun. 2015. Geochronological and geochemical constraints on the origin of clastic meta-sedimentary rocks associated with the Yuanjiacun BIF from the Lüliang Complex, North China. Lithos, 212 ~ 215: 231 ~ 246.

Wang Changle, Zhang Lianchang, Lan Caiyun, Li Hongzhong, Huang Hua. 2015&. Analysis of sedimentary facies and depositional environment of the Yuanjiacun banded iron formation in the Lüliang area, Shanxi Province. Acta Petrologica Sinica, 31(6): 1671 ~ 1693.

Wang Changqiu, Cui Wenyuan, Krner A, Nemchin A A. 1999#. The zircon isotopic age of magnetite quartzite in the Archean Jianping metamorphic complex, western Liaoning province. Chinese Science Bulletin, 44(15): 1666 ~ 1670.

Wang Shoulun, Zhang Ruihua. 1995&. U-Pb isotope age of individual zircon from biotite leptynite in the Qidashan iron deposit and its significance. Mineral Deposits, 14(3): 216 ~ 219.

Wang Wei, Wang Shijin, Liu Dunyi, Li Peiyuan, Dong Chunyan, Xie Hangqiang, Ma Mingzhu, Wan Yusheng. 2010&. Formation age of the Neoarchaean Jining Group (banded iron formation) in the western Shandong province: constraints from SHRIMP zircon U-Pb dating. Acta Petrologica Sinica, 26(4): 1175 ~ 1181.

Wang Yifei, Xu Huifang, Merino E, Konishi H. 2009. Generation of banded iron formations by internal dynamics and leaching of oceanic crust. Nature Geoscience, 2: 781 ~ 784.

Weyer S, Ionov DA. 2007. Partial melting and melt percolation in the mantle: The message from Fe isotopes. Earth and Planetary Science Letters, 259: 119 ~ 133.

Widdel F, Schnell S, Heising S, Ehrenreich A, Assmus B, Schink B. 1993. Ferrous iron oxidation by anoxygenic phototrophic bacteria. Nature, 362: 834 ~ 836.

Wilde S A, Cawood P A, Wang K Y, Nemchin A A. 2005. Granitoid evolution in the Late Archean Wutai Complex, North China Craton. Journal of Asian Earth Sciences, 24: 597 ~ 613.

Wright J, Schrader H, Holser W T. 1987. Paleoredox variations in ancient oceans recorded by rare earth elements in fossil apatite. Geochim. Cosmochim. Acta, 51: 631 ~ 644.

Wu Shiying, Zhang Daojian, Wang Kuiyang, Chen Chengye, Bai Liming. 2000. Geochemical characteristics of stable isotopes from hydrothermal chimneys in the Mariana trough, West Pacific Ocean. Chinese Journal of Oceanology and Limnology, 18: 378 ~ 384.

Yang Xiaoyong, Wang Bohua, Du Zhenbao, Wang Qicai, Wang Yuxian, Tu Zhengbiao, Zhang Wenli, Sun Weidong. 2012&. On the metamorphism of the Huoqiu Group, forming ages and mechanism of BIF and iron deposit in the Huoqiu region, southern margin of North China carton. Acta Petrologica Sinica, 28(11): 3476 ~ 3496.

Yang Xiaoyong, Liu Lei, Lee Insung, Wang Bohua, Du Zhenbao, Wang Qicai, Wang Yuxian, Sun Weidong. 2014. A review on the Huoqiu banded iron formation (BIF), southeast margin of the North China Craton: Genesis of iron deposits and implications for exploration. Ore Geology Reviews, 63: 418 ~ 443.

Yang Xiuqing. 2013&. Study on iron Ore-forming process of metamorphic terrain in Anshan—Benxi area, Liaoning province, China. Tutor: Xue Chunji, Li Houmin. Beijing: China University of Geoscicences (Beijing), Master degree thesis, 1 ~ 136.

Zhai Mingguo, Windley B F, Sills J D. 1990. Archaean gneisses amphibolites, banded iron-formation from Anshan area of Liaoning, NE China: Their geochemistry, metamorphism and petrogenesis. Precambrian Research, 46: 195 ~ 216.

Zhai Mingguo, Windley B F. 1990. The Archaean and early Proterozoic banded iron formations of North China: Their characteristics geotectonic relations, chemistry and implications for crustal growth. Precambrian Research, 48: 267 ~ 286.

Zhai Mingguo, Santosh M. 2013. Metallogeny of the North China Craton: Link with secular changes in the evolving Earth. Gondwana Research, 24: 275 ~ 297.

Zhang J, Amakawa H, Nozaki Y. 1994. The comparative behaviours of yttrium and lanthanides in the seawater of the North Pacific. Geophysical Research Letters, 21: 2677 ~ 2680.

Zhang Xiaojing, Zhang Lianchang, Xiang Peng, Wan Bo, Pirajno F. 2011. Zircon U-Pb age, Hf isotopes and geochemistry of Shuichang Algoma-type banded iron-formation, North China Craton: Constraints on the ore-forming age and tectonic setting. Gondwana Research, 20: 137 ~ 148.

Zhang Lianchang, Zhai Mingguo, Wan Yusheng, Guo Jinghui, Dai Yanpei, Wang Changle, Liu Li. 2012&. Study of the Precambrian BIF-iron deposits in the North China Craton: progresses and questions. Acta Petrologica Sinica, 28(11): 3431 ~ 3445.

Zhang Lianchang, Zhai Mingguo, Zhang Xiaojing, Xiang Peng, Dai Yanpei, Wang Changle, Franco Pirajno. 2012. Formation age and tectonic setting of the Shirengou Neoarchean banded iron deposit in eastern Hebei Province: Constraints from geochemistry and SIMS zircon U-Pb dating. Precambrian Research, 222 ~ 223: 325 ~ 338.

Zhang Zhaochong, Hou Tong, Santosh M, Li Houmin, Li Jianwei, Zhang Zuoheng, Song Xieyan, Wang Meng. 2014. Spatio-temporal distribution and tectonic settings of the major iron deposits in China: An overview. Ore Geology Reviews, 57: 247 ~ 263.

Zhao Guochun, Wilde S A, Cawood P A, Sun Min. 2001. Archean blocks and their boundaries in the North China Craton: Lithological, geochemical, structural and *P*—*T* path constraints and tectonic evolution. Precambrian Research, 107: 45 ~ 73.

Zhao Guochun, Wilde S A, Sun Min, Li Sanzhong, Li Xuping, Zhang Jian. 2008. SHRIMP U-Pb zircon ages of granitoid rocks in the Lüliang Complex: Implications for the accretion and evolution of the Trans-North China Orogen. Precambrian Research, 160: 213 ~ 226.

Zheng Mengtian, Zhang Lianchang, Wang Changle, Zhu Mingtian, Li Zhiquan, Wang Yating. 2015&. Formation age and origin of the Xingshan BIF-type iron deposit in eastern Heibei Province. Acta Petrologica Sinica, 31(6): 1636 ~ 1652.

Zhou Shitai. 1994 #. Geology of the BIF in Anshan—Benxi area. Beijing: Geological Publishing House, 1 ~ 277.

Zhou Yonggui, Chen Zhengle, Chen Bailin, Han Fengbin. 2012&. Genesis of rich and large orebody in Xingshan iron deposit of Qian'an orefield, Hebei province. Journal of Jilin University (Earth Science Edition), 42(S3): 81 ~ 92.

Zhu Mingtian, Dai Yanpei, Zhang Lianchang, Wang Changle, Liu Li. 2015. Geochronology and geochemistry of the Nanfen iron deposit in the Anshan—Benxi area, North China Craton: Implications for ~ 2.55 Ga crustal growth and the genesis of high-grade iron ores. Precambrian Research, 260: 23 ~ 38.

Ziegler K, Chadwick O A, Brzezinski M A, Kelly E F. 2005. Natural variations of δ^{30} Si ratios during progressive basalt weathering, Hawaiian Islands. Geochim. Cosmochim. Acta, 69: 4597 ~ 4610.

An Overview of Studies on Precambrian Banded Iron Formations (BIFs) in China and Abroad

DAI Yanpei[1, 2)], ZHU Yudi[3)], ZHANG Lianchang[2)], WANG Changle[2)], CHEN Chao[4)], XIU Di[4)]

1) *Chengdu Center*, *China Geological Survey*, *Chengdu*, 610081;

2) *Institute of Geology and Geophysics*, *Chinese Academy of Sciences*, *Beijing*, 100029;

3) *School of Geoscience and Technology*, *Southwest Petroleum University*, *Chengdu*, 610500;

4) *Hebei Institute of Regional Geological and Mineral Resource Survey*, *Langfang*, *Hebei*, 065000

Abstract: Banded iron formations (BIFs) were mainly formed in the early Precambrian (3.8 ~ 1.8Ga); they record some important information about the evolution of early Earth and contain very large amounts of iron ores. This paper summarizes the significant advances and open issues on the BIF-related studies in China and abroad: ① the statistics and comparisons indicate that the BIF deposition was associated with momentous geological events, such as mantle plumes and crustal growth; ② the REE and Nd isotope show that Fe precipitated from marine seawater with minor high-temperature hydrothermal component in the proportion of 1:1000; ③ most of BIFs have no Ce anomalies with enrichment in $\delta^{57}Fe_{IRMM}$, implying that the paleo-ocean was in low abundances of O_2 and thus Fe^{2+} could not be oxidized; ④ some key scientific problems have not been resolved, such as the source of Si, precipitation mechanism and genesis of bands; ⑤ BIFs in the North China Craton primarily occurred at about 2.54 Ga; however, some issues need to research deeply, such as the BIF types, formation ages and genesis of high-grade iron ores. We propose that the comparative studies on typical BIFs and applications of advanced measuring techniques are helpful to understand the precise procedures of BIF deposition and early evolution of old cratons.

Keywords: banded iron formations; source of materials; precipitation mechanism; depositional environment; genesis of bands; formation age

Acknowledgements: This work was supported by Projects 973 of National Key Basic Research Program (No. 2012CB416601), Scientific Research Project of Education Department of Sichuan Province (No. 15ZB0058) and Youth Science Fund Project of Chengdu Center, China Geological Survey (No. [2015]-05). We thank Professor WAN Yusheng and another anonymous reviewer for their valuable suggestions on this manuscript.

First author: DAI Yanpei, male, born in 1986. Engineer, a doctor of science, mainly engages in economic geology. Email: diyeplas@foxmail.com.

Manuscript received on: 2015-05-07; Accepted on: 2015-12-04; Edited by: ZHANG Yuxu.

Doi: 10.16509/j.georeview.2016.03.015